Doctoral Thesis
博士論文
(Abridged Version)

Spatial distribution and formation of fluvial knickzones in central Japan extracted using multi-resolution Digital Elevation Models (DEMs) and GIS-based tools

（多解像度のデジタル標高モデルと GIS のツールを用いて抽出した中部日本の河川遷急区間の分布と形成）

Tuba Zahra
トゥバ　ザヘラ

March, 2017
2017 年 3 月

Department of Natural Environmental Studies,
Graduate School of Frontier Sciences,
The University of Tokyo
東京大学大学院新領域創成科学研究科
自然環境学専攻

Spatial distribution and formation of fluvial knickzones in central Japan extracted using multi-resolution Digital Elevation Models (DEMs) and GIS-based tools

多解像度のデジタル標高モデルと GIS のツールを用いて抽出した中部日本の河川遷急区間の分布と形成

by

Tuba Zahra

Thesis submitted for the degree of Doctor of Science

Department of Natural Environmental Studies (NENV)
Graduate School of Frontier Sciences (GSFS)
The University of Tokyo

March, 2017

Supervisor
Professor Takashi Oguchi

東京大学
THE UNIVERSITY OF TOKYO

This Thesis was made possible by the Grant-in-Aid provided by Japanese Government (Monbukagakusho:MEXT) Scholarship 2011, GSFS Grant for Ph.D. Research Program, 2014 & 2015 and the JASSO fellowship 2015-2017 as a result of considering the author's academic research achievement.

Author's Declaration:

I do hereby pledge that I have followed the standards regarding scientific research set forth in the Code of Conduct for Scientific Research of The University of Tokyo and the Graduate School of Frontier Sciences Guidelines for Research Ethics.

Name _____

(Tuba Zahra)

Abstract

Extraction of knickpoints or knickzones from a Digital Elevation Model (DEM) has gained immense significance owing to the increasing implications of knickzones on landform development. However, existing methods for knickzone extraction tend to be subjective or require time-intensive data processing. This study uses a newly proposed Knickzone Extraction Tool (KET) and the Semi-Automatic Knickzone Extraction (SAKE) method for the extraction of knickzones. KET, deployed in the form of an ArcGIS toolset, automates the process of knickzone extraction and is both fast and more user-friendly. A comparative analysis of KET, SAKE and other contemporary knickzone identification techniques was also conducted. The results from 10-m and 50-m grid DEMs of two geologically different case study areas (mountainous watersheds of the northern Japanese Alps in Gifu and and the Kii Peninsula, respectively) were examined to determine the influence of grid resolution and scale on the extraction of knickzones. In addition, the geologically different study areas determine the transferability of the KET in the extraction of prominent knickzones. Finally, through the results of case studies of the mountainous watersheds in central Japan, the relationship between knickzone distribution and its morphometric characteristics are also examined.

Three contemporary tools, the Stream Profiler Tool (SPT), the GIS Knickfinder (GKF) tool and the SAKE method were used to identify or extract knickzones from a 10-m DEM (SAKE10) of a mountainous watershed in Gifu, resulting in 113, 16 and 141 knickzones, respectively. KET, a new tool was conceptualized and applied to the same study area that identified 189 knickzones using the threshold value 1.42×10^{-5} m^{-1} (KET1) from Hayakawa and Oguchi (2006, 2009). Another threshold value of 1.92×10^{-4} m^{-1} using the mean and standard deviation of relative river steepness (R_d) at the measurement length of d for all the bedrock reaches in the study area, following the guideline of Hayakawa and Oguchi (2006, 2009) was also used. This resulted in 20 knickzones (KET2). The results from the four methods using the 10-m DEM are also

compared with the knickzones identified by Hayakawa and Oguchi (2006, 2009) who used the SAKE method and a 50-m DEM (SAKE50) since the study contains field validated knickzones. The transferability of KET was tested on 10-m and 50-m DEMs of a mountainous watershed of thw Kii Peninsula that successfully resulted in 99 and 80 knickzones, respectively using the SAKE method, while, 13 and 46 knickzones, respectively using KET. The study also analyzed the locational intersection between knickzones. In other words, an analysis of the intersection of knickzones within a certain distance was conducted. For the intersection distance, six values were used: 15, 30, 45, 60, 75, and 90 m. The degree of intersection is highest for distances of 90 m, considerably good results are also found at 45 m. The rates of increase of the percentage of intersection from 45 to 60 m, 60 to 75 m, and 75 to 90 m distance are approximately 1.15%, 0.39%, and 0.77%, respectively.

The results indicate that KET is useful for extracting knickzones by detecting anomalies in the stream length gradient. It performs well in detecting prominent knickzones in the upstream areas, although it is dependent on the applied threshold values, as is the case for the SAKE method.

Finally, the analysis of the frequency of knickzones computed for each class of elevation, distance from the watershed outlet, drainage area and stream gradient for all the rivers reveals high frequency in two elevation zones in Gifu: moderate elevations of 1600–2000 m and the other at higher elevations of 2200–2400 m. The high elevation region lies within approximately 10–15 km from the river head and a local maxima at about 50–70 km distance from the watershed outlet for all the methods. The frequency of knickzones for most methods reveals an abundance of knickzones in the smallest drainage area (10 km^2), although SAKE10 gives the most abundant knickzones between 10–20 km^2, and KET2 does not give a clear trend because the number of knickzones is small. Whereas, for Kii the frequency of knickzones computed for each class of elevation, normalized distance upstream and drainage area for all the rivers reveals

high frequency in elevations between 1000–1600 m that consist of 20% of the upstream areas of the rivers. Frequency of knickzones are abundant in small drainage areas of 10–30 km^2 with higher drainage areas associated with the 50-m DEM. In both study areas knickzones are abundant in the upstream reaches which can be attributed to strong hydraulic action in steep reaches. Although the average watershed slope and hypsometry are very similar for both the areas, the river gradient differs, 0.036 m m^{-1} for Gifu and 0.011m m^{-1} for Kii for d = 750 m. This suggests that despite the dominance of similar V-shaped valleys, the lower river gradient in Kii leads to reduced hydraulic action, resulting in much less knickzones.

Knickzone characteristics in terms of underlying rock types was also analyzed individually for Gifu and Kii. In Gifu, abundance of knickzones in the upper reaches is influenced by irregular relief and slope of the dominant volcanic rock. The river gradient d = 750 m, for volcanic, accretionary, sedimentary and plutonic rocks are 4.80×10^{-2}, 2.90×10^{-2}, 1.05×10^{-2} and 1.18×10^{-2} m m^{-1}, respectively. The plutonic and sedimentary rocks have high frequency owing to a short river stretch of 5 km distance for the former and a longer draining river of ca. 230. 6 km for the latter, but with fewer knickzones. In Kii, river action with the combined influence of its coastal location and accretionary rock complex contributes to abundance of knickzones in the upstream reaches. But river profiles are more complex with abundant knickzones in both the areas. This is refelected by the knickzone frequency of 0.2 km^{-1} in Gifu while that of 0.03 km^{-1} in Kii. The abundance of knickzones are mainly influenced by the irregular relief and slope characteristics that correlate well with hydraulic action in upstream reaches in Japan.

Table of contents

List of figures

List of tables

1. Introduction

Knickzones or knickpoints as conspicuous breaks-in-slope along a river longitudinal profile, often characterized by steepening channel gradient (Goudie, 2004; Matthews, 2013) have drawn much interest in the study of landform processes. Referred as perturbations or convexities along the longitudinal channel profiles, propagation of knickzones as a process of bedrock incision deserves geomorphological attention (Seidl and Dietrich, 1992; Seidl, 1993; Howard et al., 1994; Zaprowski et al., 2001). Knickzones that develop along the stream thalwegs or bedrocks influence the shape and trend of the longitudinal channel profiles. The controls of bedrock geology such as lithology, stratigraphy and structure on knickzone origin, morphology and evolution are the key components in geomorphic research (Pederson and Tresslor, 2012). In addition, regional knickzone distribution maps are not only valuable resources for fluvial geomorphology (Heimsath et al., 2001; Hayakawa and Matsukura, 2002) but are recently being incorporated into mass-wasting inventories for improved detection of debris flow (Lyons et al., 2014). Besides, knickzones as climatic markers (Zeuner, 1945; Zhang et al., 2011) present new opportunities of research in quantifying the morphology of erosional shorelines in Pleistocene lakes (Hare et al., 2001; Jewell, 2016).

Although knickzone research has drawn much interest in the study of landforms, much of the studies have been conducted with respect to bedrock/river longitudinal profiles. This is because bedrock channels are sensitive to tectonics and act as primary agents that diffuse signals of climatic or tectonic changes to the landscape (Merrits and Vincent, 1989, Whipple, 2004). Analysis of bedrock river profile acts as an important tool for interpreting landscape signals. A number of studies have successfully used profile analysis to determine patterns of active tectonic deformation within the underlying region (Hack, 1957, 1973; Seeber and Gornitz,

1983; Keller, 1986; Lavé and Avouac, 2000, 2001). In stream-profile analysis, morphological indices such as stream gradient and slope-area analysis have also been applied in landscape evolution studies (Tarboten et al., 1989; Sklar and Dietrich, 1998; Snyder et al., 2000; Lin and Oguchi, 2004; Wobus et al., 2006a; Kirby and Whipple, 2012).

In due course, knickzone research has evolved from a rather descriptive study (Gilbert, 1877; Penck, 1925; Davis, 1932) corresponding to bedrock channel evolution focusing on longitudinal profile analysis, into an independent research discipline contributing not only to geomorphic, geologic and hydrological sciences but also to other environmental disciplines (Hare et al., 2001). This chapter includes the definition of knickzones and its types, the evolving trends in knickzone research focusing on their formation, process and rates of evolution, and the current progress in computer-based simulations or modeling. Finally, a brief outline about the current knickzone research in Japan is followed by the problem statement and objectives of this study.

1.1. Knickpoint/Knickzone definition and types

1.1.1. Definitions

The word *knickpunkte* or *knickpoint* originates from Penck's (1925) treppen concept that discusses the origin of knickpoints and its influence on the evolution of the piedmont plain. The theory, though debated, defines knickpoints as convex breaks-in-slope that separate the upper and the lower graded reaches in a longitudinal profile, draining over homogenous rocks that are continuously undergoing accelerated uplift. Macar (1934) defines knickpoint as irregularities in the longitudinal profile of a river formed by differences in rock resistance and rejuvenation. American Geological Institute Glossary (1957) include of two spellings and definitions: a) Nickpoint – the point of interruption of a stream profile at the head of a second-cycle valley according to the treppen concept; and b) Knickpoint – points of abrupt changes in the longitudinal profile of a stream (Brush and Wolman, 1960). According to Schumm et al. (1987),

knickpoints represent abrupt topographic breaks in longitudinal channel profiles and are generally considered to be non-equilibrium landforms. Howard et al. (1994) defines knickpoint as a relatively steep local reach between lower gradient sections produced either by tectonic deformation, base level changes, or variable rock resistance. While a knickzone is an extended steep reach in a fluvial long profile depending on its length, a knickpoint is a visually distinct point on the longitudinal profile (Gardner, 1983; Miller, 1991; Downs and Simons, 2001; Hayakawa and Oguchi, 2006, 2009) and in the laboratory knickpoints are often termed as headcuts (Bennett, 1999; Rengers and Tucker, 2014). Note that in this study the word knickzone is used as a relatively steep gradient along a river that includes knickpoints and associated similar features such as rapids, cascades, waterfalls and gorge heads regardless of their scales.

1.1.2. Knickzone types

Based on the mode of development that determine the absence or presence of morphological features, classification of knickpoint dates back to 1976 when Holland and Pickup (1976) identified three major knickpoints in different rock types. The major types with their morphological characteristics are: a) stepped knickpoints – structural in origin and resulting as a function of the underlying lithology of a river bed to its thickness, often with a characteristic vertical face and plunge pool; b) rotating knickpoints – elongated over-steepened reaches formed when a knickpoint reaches its extinction; and c) minor erosional knickpoints – that are agents of incision formed on the river beds.

Tinkler (2004) (in the encyclopaedia by Goudie, 2004) classified knickpoints into two: a) headward retreating knickpoints synonymous to waterfalls and hanging valleys. In this case, the steepened valley walls collapse by mechanical failure and stress release (Philbrick, 1970). Or, stepped knickpoints, that retain a vertical face due to enhanced groundwater drainage and/or cutting the valley walls by stream erosion; and b) rotating knickpoints that retreat when the

headwall in a weak material is unable to maintain the cap-rock and flattens as it migrates upstream (Stein and Julien, 1993).

Another classification of knickpoint (Haviv et al., 2010) distinguishes it into two major types: a) break-in-gradient knickpoint – found in both cohesive and non-cohesive substrates and, b) break-in-elevation knickpoint – only available in cohesive substrates, which is further classified into two: i) break-in-elevation knickpoint where the height is less than the flow depth and its step-like evolution is governed by hydrodynamics; and ii) vertical knickpoints where the height is greater than the flow depth and the processes of weathering and gravitation are dominant. Both types are found in homogeneous and resistant cap-rocks.

It must be noted that a genetic classification of knickpoints or knickzones may not be only necessary because several processes may lead to their formation and successive propagation. But a morphogenetic classification of knickzones is required (Castillo-Rodríguez, 2011) because knickzones can occur in both alluvial and bedrock rivers, and in cohesive and non-cohesive materials (Holland and Pickup, 1976; Gardner, 1983; Wolman, 1987; Frankel et al., 2007).

Section 1.2. Evolving trends in knickzone research and subsections have been removed for future publication.

1.3. Knickzone research in Japan

In Japan, the heavily dissected steep mountain watersheds that are often influenced by rapid tectonic uplift are frequented by storms that are associated with active erosion. Although the Japanese Alps are considered to be in a state of dynamic equilibrium (Ohmori, 1978; Katsube and Oguchi, 1999), the bedrock rivers are marked by the presence of knickpoints/knickzones, often accompanied by waterfalls and poses a contradiction to the dynamic equilibrium state of the rivers (Hayakawa and Matsukura, 2003a; Hayakawa, 2007; Hayakawa et al., 2008; Hayakawa and Oguchi, 2013). Several researches have mentioned about knickpoints/knickzones in relation to Japan (Mino, 1958; Okunishi, 1974; Sakai, 1998) but very

few researches have actually addressed the problem of detection of knickzones (Hayakawa and Oguchi, 2006, 2009), causes of their formation and their distribution (Hayakawa and Oguchi, 2013). Knickzone research is still evolving with current studies in association with slope deformations (Hiraishi et al., 2011) and mass-wasting (Chigira et al., 2015), with more scope in future.

1.4. Existing problems and the aims of this thesis

Traditionally, knickzones were identified by visual inspection of river longitudinal profiles or their slope-area relationships (Whipple and Tucker, 1999; Phillips et al., 2010; Ambili and Narayana, 2014; Antón, et al., 2014). Such manual interpretations make the studies subjective. Field observations and surveys for morphologically identifying knickzones (Sakai, 1998; Zaprowski, et al., 2001; Crosby and Whipple, 2006) are also tedious. Therefore, some studies have pursued automated approaches for knickzone extraction. For example, Whipple et al. (2007) applied the Stream Profiler Tool (SPT), and Hill and Stewart (2014) used local changes in the normalized steepness index (k_{sn}) from upstream to downstream.

Another method of knickzone extraction based on changes in stream gradient with respect to spatial scale was proposed by Hayakawa and Oguchi (2006) that used a DEM and GIS. The Semi-Automatic Knickzone Extraction (SAKE) method (Hayakawa and Oguchi, 2006, 2009) consisted of a vector-based semi-automated procedure that required somewhat time-intensive data processing because of the independent use of GIS and spreadsheet software.

Owing to the existing challenges in deriving a regional scale knickzone distribution map, automating the different methods of knickzone extraction is still an emerging field of research. This study uses a newly proposed Knickzone Extraction Tool (KET), the SAKE method and some other contemporary tools for the extraction of knickzones. Although applications of knickzones has been emerging in various research areas, yet very few studies have considered

a comparative analysis of knickzone identification techniques. Keeping this in mind a comparative analysis of the KET, SAKE and other contemporary knickzone identification techniques was conducted. In addition, availability of improved high resolution DEMs has led to comparative studies with respect to DEM grid resolution and scale as a mandatory subject to be explored in the context of knickzones.

The following specific objectives were defined:

- Comparative analysis and extraction of knickzones using contemporary knickzone identification techniques.
- Study the effects of DEM grid size and scale on knickzone distribution in both the study areas.
- Analyse the influence of thresholds on knickzone location by different DEM grid resolutions.
- Discuss the influence of rock types on knickzone distribution and properties.
- Assess the distribution of knickzones in two geologically different watersheds (Gifu and Kii) of central Japan.

1.5. Structure of the thesis

This research uses different knickzone identification tools and 10-m and a 50-m grid DEMs for two case study areas. The relationship between knickzone distribution and its morphometric characteristics are also examined. The chapters of the thesis are organized in the best possible manner to present the integrated idea.

Chapter 1 presents the significance of knickzone as an independent research discipline, provides the definition and types of knickzones, and describes the evolving trends in knickzone research, states the current research problems that define the research objectives followed by summarising the structure of the thesis. Chapter 2 introduces the case study, areas from central Japan, selected for this research with details on their geo-environmental conditions. Chapter 3 describes the contemporary knickzone identification techniques and introduces the newly proposed KET tool along with other methods adopted in this study. Chapters 4, and 5 includes the results obtained by the use of the methods described in Chapter 3. Chapter 6 discusses the results in order to associate the observations with their causes. Chapter 7 summarises and synthesizes the results and discussion from Chapters 4 to 6, providing general conclusions, and an outlook for the use of KET as an effective tool for identification of prominent knickzones. This chapter also provides details of knickzone evolution in two geologically different areas of Japan thereby concluding the research with future recommendations.

2. Study Area and Data

The study comprises of analyses conducted in two case studies in geological and environmental settings. The first case study in Gifu is used for the application of all the methods of knickzone extraction and comparison of the results; while the second case study in Kii is used to test the transferability of the SAKE method and KET. Both the analyses uses 10-m and 50-m DEMs respectively. Both the study areas are also used for comparison of the knickzone formation processes.

2.1. Case studies

2.1.1. Gifu

The case study area to compare the new and existing methods is a mountainous region of the southwestern side of the northern Japanese Alps, Gifu Prefecture, Japan (Figure 2-1). It consists of the southern slopes of Mount Norikura in the north and the north-western slopes of Mount Ontake on its west that comprises parts of the Hida mountains (>3000 m), that are the highest mountain ranges in Japan (Ide, 2001). Mount Ontake witnessed a volcanic eruption earlier in 2014 and its north-western slopes are marked by many mass-wasting events. The watershed is a part of the Takayama and Gero areas of Gifu and is drained by the tributaries of the Hida river flowing southwards.

The area consists of various rocks mainly accretionary complex and volcanic up to early Pleistocene, and is associated with varying topography (Sohma and Kunugiza, 1993). Data for the nearest weather station in Takayama City shows that the region receives precipitation in the form of winter snow from December to March (a total of 2860 mm in 108 days, according to JMA, 2014) and summer rain, with an annual precipitation of 2097 mm (JMA, 2014). In the

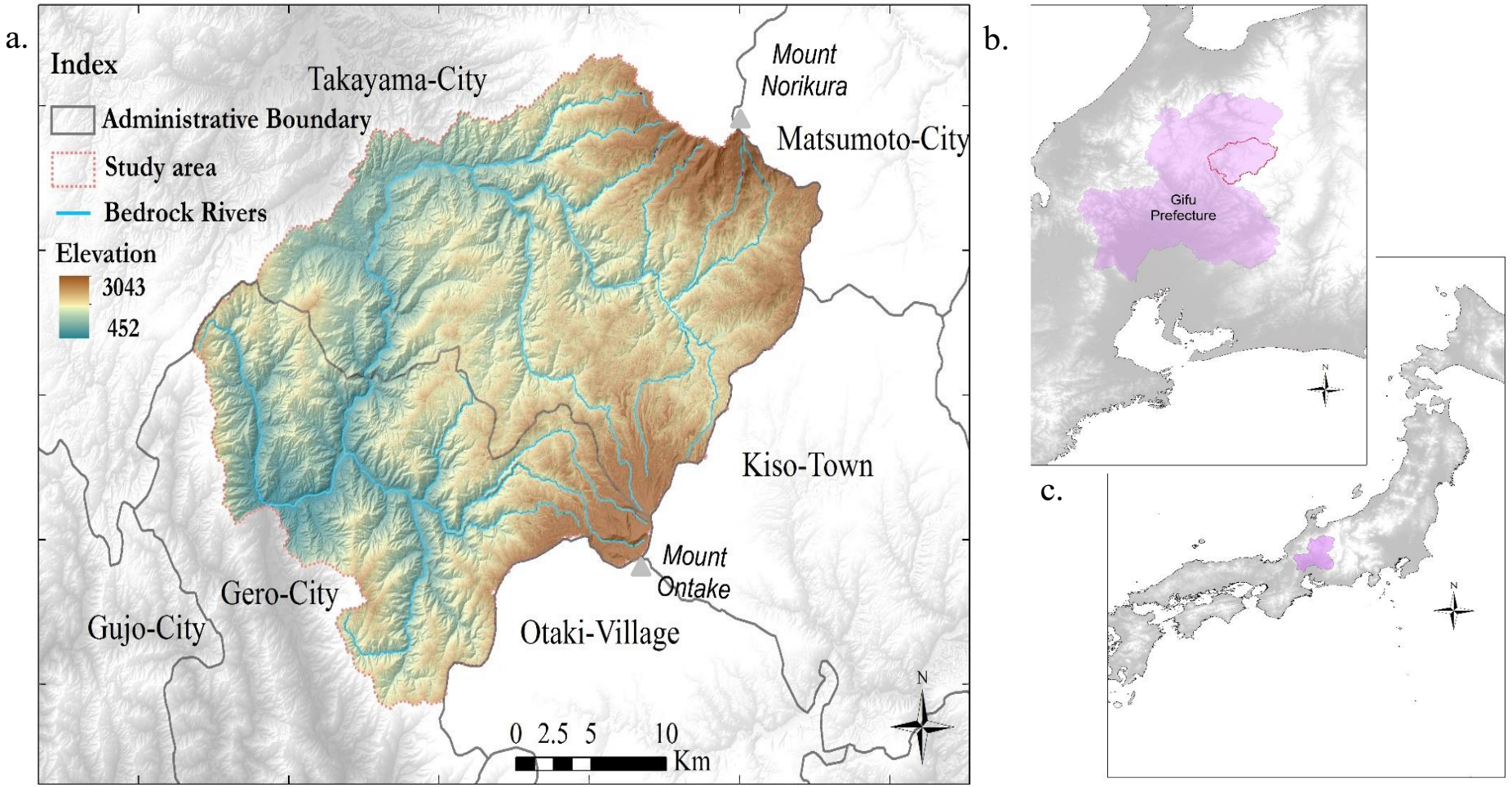

Figure 2-1: Case study area in Gifu. A. Studied watershed b. Gifu Prefecture with the Gero watershed; and c. Map of Japan with the Gifu Prefecture.

watershed a number of waterfalls such as the Neo-no-taki falls and the Mitsudaki falls also occur and human intervention is limited. Therefore, the Gero watershed seems to be suitable for knickzone analysis.

2.1.2. Kii

The second case study (Figure 2-2) located in the Kii Peninsula is surrounded by the Mie, Nara and Wakayama Prefectures to the east, north, and south-western parts respectively. The Omine Mountain ranges with the highest peak of about 1912 m forms the north and central parts, while Mount Obako and Mount Odaigaharazan bordering the eastern and the western parts of the study area comprises the Kii Mountain Ranges. The central part of the Kii Mountains is drained by the Kumano River and its tributaries flowing from north to south. It consists of three sections: the Tenno-gawa, the Totsu-kawa and the Kumano-gawa, but in this research the entire river is referred as the Kumano River (Chigira et al., 2013) and the watershed, as the Kumano watershed. Hiraishi and Chigira (2011) found paleosurface remnants at higher elevations forming inner gorges, namely the Doryokyo gorge, along the Kumano River.

The area is underlain by the Cretaceous to Neogene Shimanto accretionary complex rocks with minor occurrences of Miocene granite and sedimentary rocks. (Yonekura, 1968; Chigira et al., 2015). Heavy rainfalls are caused by typhoons and polar fronts during the summer monsoon (Saito and Matsuyama, 2012). Data for the nearest weather stations at Tenkawa, Mount Gomudan and Miyagawa shows the annual precipitation of 2184.0, 3015.5 and 3371.5 mm (JMA, 2014), respectively.

The distinctly different topography and geological setting of the Kumano watershed in the Kii Peninsula and the Gero watershed in Gifu seems to be suitable for a comparative investigation of knickzones.

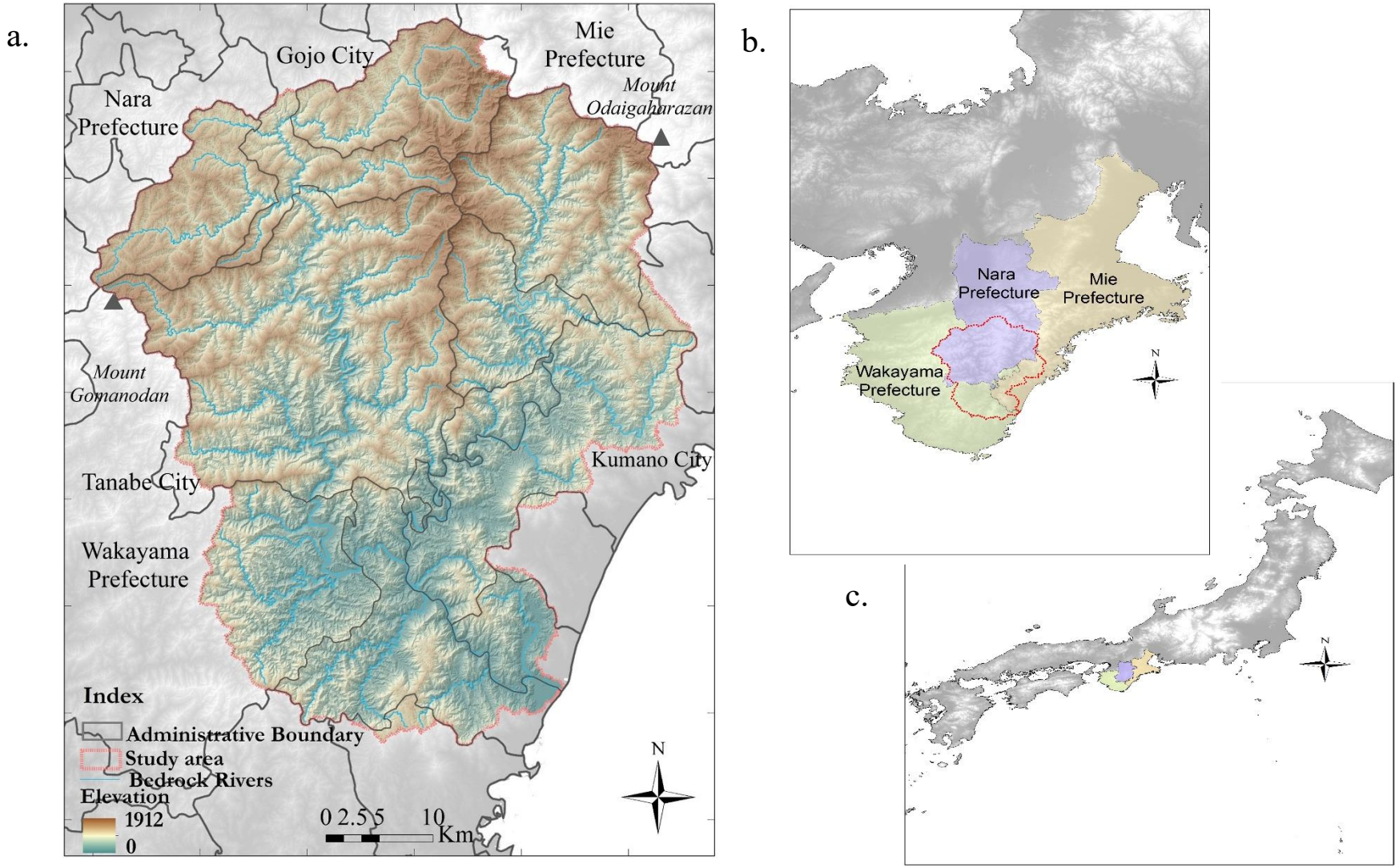

Figure 2-2: Case study area in the Kii Peninsula. a. Studied watershed; b. Prefectures with the Kumano watershed; and c. Map of Japan with the Prefectures.

2.2. Data used

A 10-m DEM from the Hokkaido Chizu Corporation, Asahikawa, Japan with a UTM Projection (zones 53N and 54N) was used to run all the contemporary knickzone identification methods. While a 50-m DEM from the Geospatial Information Authority (GSI) of Japan was also used for the Kumano watershed to run the KET and check the transferability of the tool. Both the 10-m and 50-m DEMs were filled, and water flow direction, drainage area and stream networks were identified from the filled DEMs. Slope angles and hypsometric integrals were also calculated from both the DEMs for both the study areas.

A vector map of all the bedrock rivers in Japan (National Institute of Industrial Science and Technology, 2012) was used to identify bedrocks in the respective study areas and identify knickzones along them using all the methods. Curvature values were also calculated for each of the bedrock rivers. The total length of the bedrock rivers studied in Gifu is 742 km, while the total length of the bedrock rivers analysed in Kii is 3167 km. A digital vector map of dam locations in Japan (National Land Numerical Information, the 2009 version) was used to avoid mis-identification of dams as knickzones. In addition, database of knickzone distribution using a 50-m DEM from Hayakawa and Oguchi (2006, 2009) was also used to extract knickzones for validating the knickzones in the study areas as some the database consisted of some field-verified knickzones.

The geological information of the study areas is based on the seamless digital geological maps (scale: 1: 200,000; 2013) provided by the Geological Survey Institute (GSI) of Japan. The complex geological units in the map were classified into four major rock types: sedimentary, accretionary complex, volcanic and plutonic. Grid data for mean annual precipitation for 1953–1982 with a 1-km cell size was used from the Digital National Land Information (Ministry of Land, Infrastructure and Transport, 1988) as the climatic database.

Finally, the topographic, climatic and geologic data were summarized for both the case studies. The topographic variables include mean river trend gradient (values for d = 750), mean elevation and standard deviation of elevation for local relief and the mean slope angle as they are often related to denudation rates (Ahnert, 1970; Ohmori, 1978; Wakamatsu et al., 2005). The percentage of knickzones for four rock types, along the riverbed were also calculated to represent the influence of lithology.

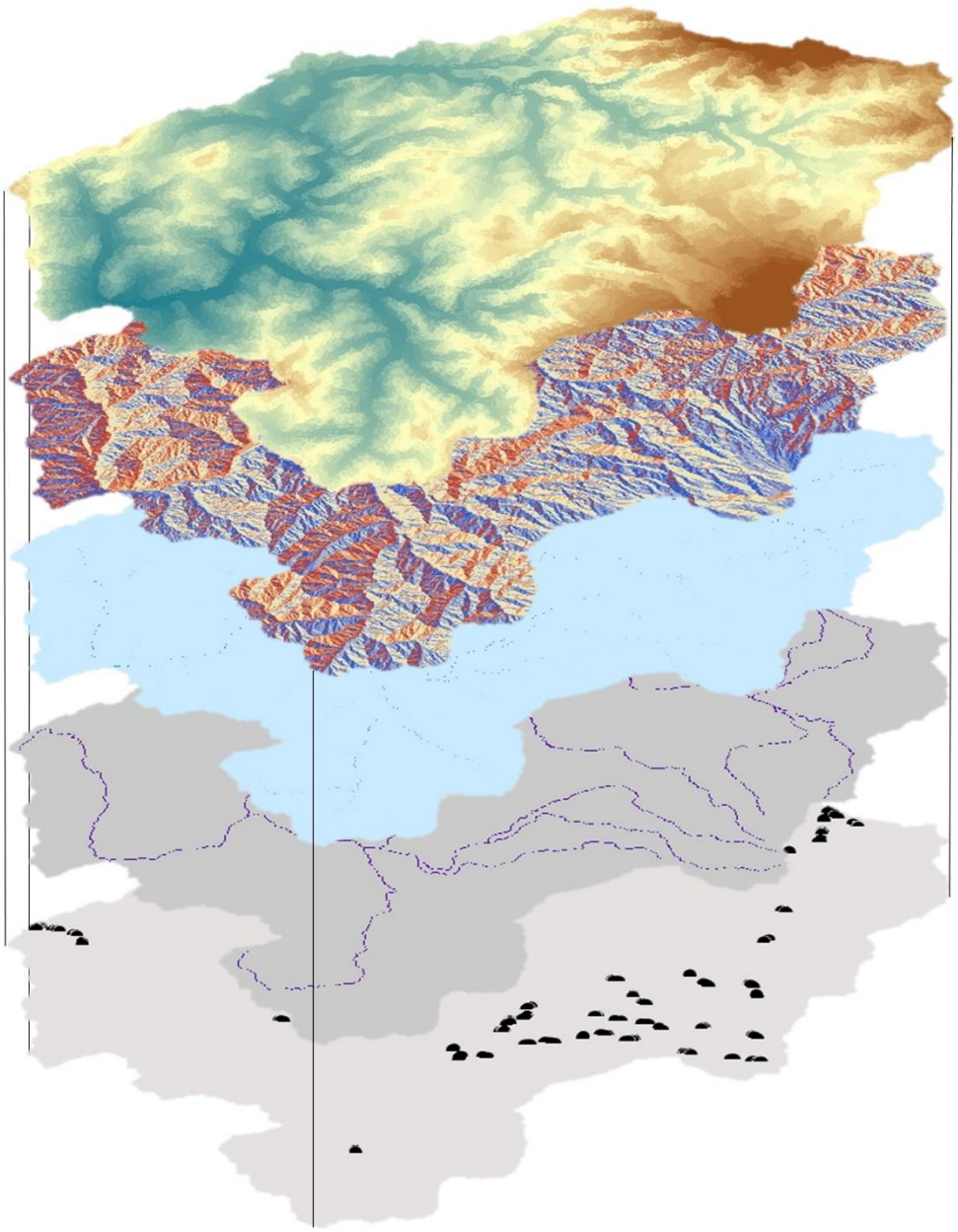

Figure 2-3: Basic data for the Gero watershed in Gifu; Layers from top to bottom: sink-filled DEM, flow direction, flow accumulation, bedrock rivers, knickzones from Hayakawa and Oguchi (2006).

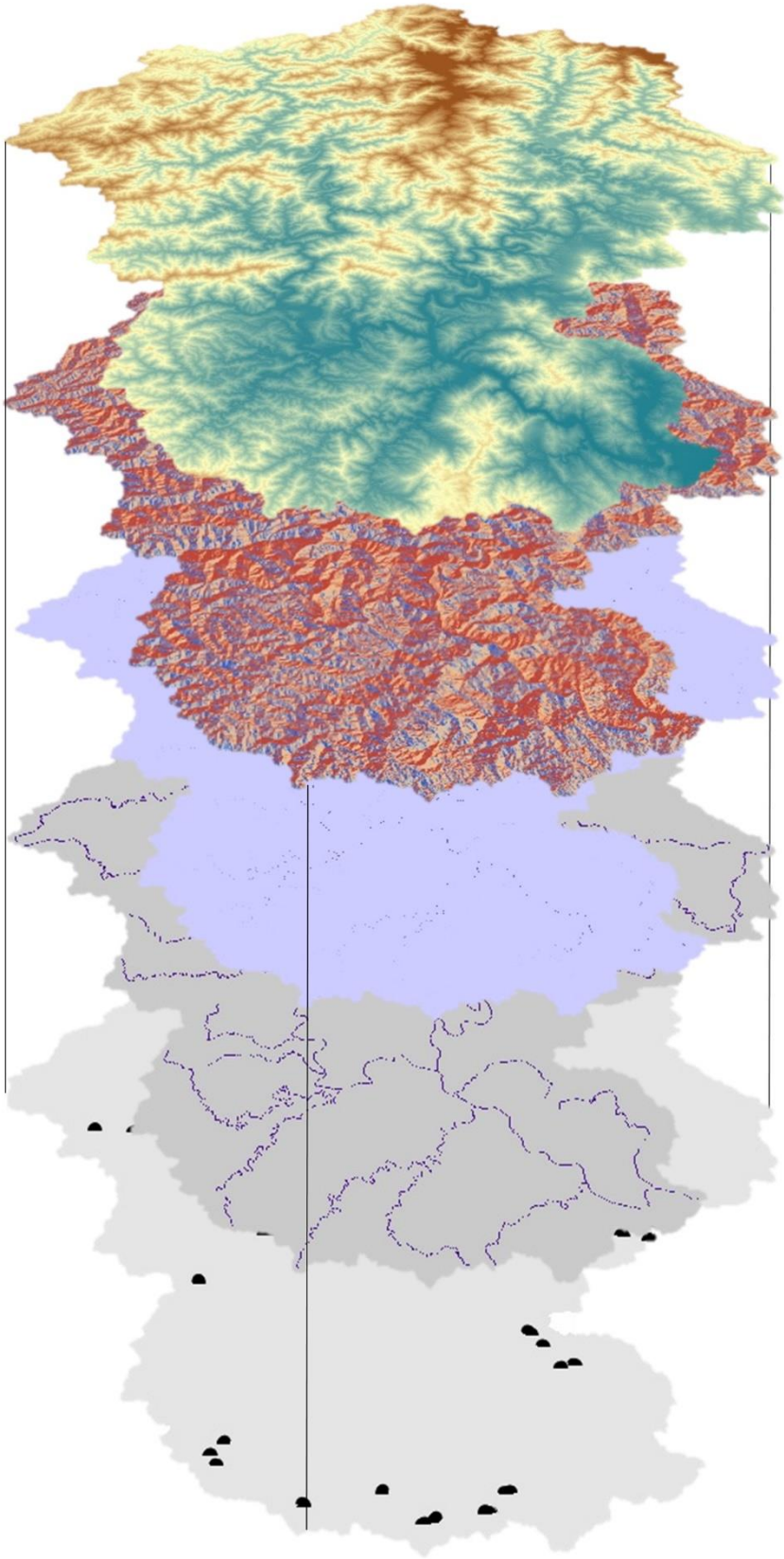

Figure 2-4: Basic data for the Kumano watershed in Kii; Layers from top to bottom: sink-filled DEM, flow direction, flow accumulation, bedrock rivers, knickzones from Hayakawa and Oguchi (2006).

3. Methods of Automated Knickzone Extraction and Analyses

This section briefly explains the existing tools or methods for knickzone extraction and comprises of two parts, Section 3.1 and 3.2. The former explains the existing methods of knickzone extraction that are popularly used and/or are in use, while the latter introduces KET. Application of the different knickzone extraction methods to the case study areas are detailed in Section 3.3 that exemplify the criteria used for identifying knickzones and their general and form properties. Section 3.4 depicts the steps for identifying knickzones from different DEM grid resolution and the multi-scale stream gradients. Besides, in order to examine the formation of identified knickzones, their abundance and form are analysed in relation to the different rock types. The final section (Section 3.5) includes the vector- and raster-based methods applied in an attempt to quantify the locational accuracy of knickzones in both the study areas, respectively.

3.1. Existing methods

The existing methods include: the SPT (Kirby and Whipple, 2001; Whipple et al., 2007) the GIS-Knickfinder (GKF; Rengers, 2012), and SAKE (Hayakawa and Oguchi, 2006). They are based on three distinct geomorphic properties: slope-area, slope-curvature, and stream gradient, respectively.

3.1.1. Stream Profiler Tool (SPT)

Based on the slope-area approach, SPT uses ArcGIS (9x and 10x) and MATLAB (R2012a and later versions) to analyze the steepness index and concavity of river profiles (Whipple et al.,

2007). The knickzones are thereby determined from an evaluation of the steepness index. The basic equation underlying the tool is:

$$S = k_s A^{-\theta} \qquad \text{Equation (1)}$$

where S is the local channel slope, A the upstream drainage area, k_s the steepness index, and θ is the dimensionless concavity index of the curve. This relationship is known as the Flint's (1974) Law. k_s is used to identify knickzones as anomalies (deviations) from the trend of the river longitudinal profile. Although SPT is widely applied to study the effects of tectonics, it is time intensive. SPT uses the built-in hydrology and surface tools of ArcGIS (9x and 10x) for extracting the drainage components of flow direction, flow accumulation, catchment area, and other attributes such as channel slope, followed by visually interpreting plots of channel parameters to demarcate knickzones.

3.1.2. GIS-Knickfinder (GKF)

Based on ArcGIS (10x) and Python libraries, GKF uses the slope-curvature approach applied to the entire raster layer instead of analyzing stream profiles individually (Rengers, 2012). The tool contains a set of algorithms related to drainage area and plan curvature. Knickzones (referred to as head-cuts in the tool) are identified as pixels with a curvature less than a certain threshold and a drainage area greater than a certain threshold.

The curvature threshold is the key to identifying knickzones based on terrain shape, whereas the drainage area threshold is used to exclude knickzones that are not along the main channel. The curvature values for a hilly area with moderate relief vary between −0.5 and 0.5, whereas for steep, rugged mountains (extreme relief), the values vary between −4 and 4 (Whipple, 2004; Francis Rengers, personal communication). Curvature values may exceed these ranges for

different areas depending on the topographical characteristics. The knickzones for each bedrock river can then be extracted by overlaying the vector line data showing bedrock rivers.

3.1.3. Semi-Automatic Knickzone Extraction (SAKE) method

The SAKE method (Hayakawa and Oguchi, 2006) is based on the assumption that the slope gradient along a river changes with measurement length, and a locally steep segment of the riverbed is considered a knickzone. The gradient of a river reach is:

$$G_d = \Delta z / \Delta d = e_1 - e_2 / \Delta d \qquad \text{Equation (2)}$$

where e_1 is the riverbed elevation $d/2$ upstream of a measuring point along a stream, e_2 is the riverbed elevation $d/2$ downstream, G_d (m m^{-1}) is the stream gradient at the measuring point,

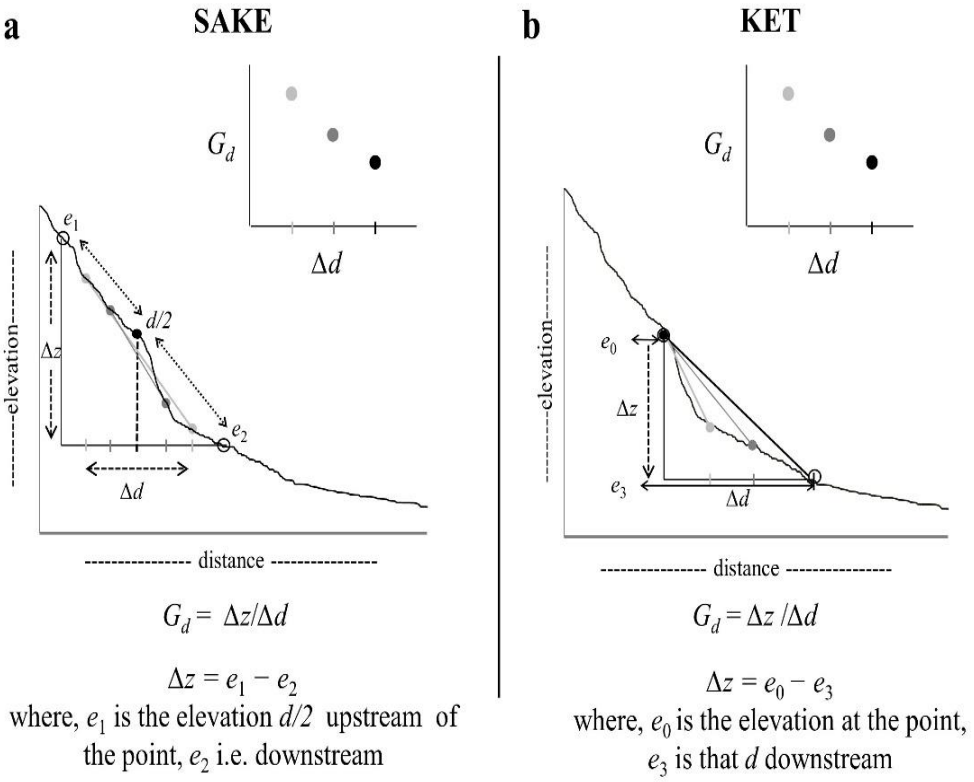

Figure 3-1: Illustrated explanation highlighting the difference between SAKE and KET methods. SAKE considers both the upstream (e_1) and the downstream (e_2) elevations that are $d/2$ apart, whereas KET uses the elevation at the point e_0 and d downstream at point e_3

and d (m) is the variable measurement distance (Figure 3-1a). SAKE calculates the scale-dependent change in G_d (m m^{-1}) by solving a linear regression equation:

$$G_d = ad + b \qquad \text{Equation (3)}$$

where d is the multi-scale measurement length, a is the regression coefficient, and b is the intercept. The relative steepness index R_d is then defined as:

$$R_d = -a \qquad \text{Equation (4),}$$

which represents the rate of gradient decrease with increasing d. R_d shows how steep the point is locally compared to the trend of the stream gradient averaged over a longer d, and a threshold of R_d can be defined for identification of knickzones. An average of the standard deviations of R_d for all the rivers in a region is then used as the threshold (Hayakawa and Oguchi, 2006).

SAKE has been applied for a regional scale analysis, and it has also been used to provide data on knickzone properties such as height, length, and gradient. These properties have been studied in relation to the altitude, upstream distance, drainage area, and geology to understand factors controlling knickzone formation (Hayakawa and Oguchi, 2006; Yunus, 2015; Yunus, 2016; Yunus et al., 2016). However, wider application of SAKE requires technical improvement, because it requires time-intensive data processing resulting from the separate use of ArcGIS (10x) and spreadsheet software.

3.2. New method: Knickzone Extraction Tool (KET)

KET, a new raster-based Python script deployed in the form of an ArcGIS toolset, is proposed in this study. It intends to automate the process of SAKE for faster and more user-friendly knickzone extraction, but there are some differences from SAKE for technical reasons. For example, KET calculates G_d using the following equation:

$$G_d = \Delta z / \Delta d = e_0 - e_3 / \Delta d \qquad \text{Equation (5).}$$

SAKE considers both the upstream and downstream elevations $d/2$ apart (Figure 3-1a, Equation 2), whereas KET uses the elevation at the point e_0 and d downstream at point e_3 (Figure 3-1b). The method of SAKE considers both the upstream and downstream elevations for detecting a locally steep segment; this method, however, is inapplicable to the uppermost section of the river. KET is applicable from the top of the river, so it requires a simple algorithm that follows the flow direction and is free from the ambiguity of determining the uppermost point of the river.

This program, available as an ArcGIS toolset, utilizes the built-in spatial analyst functions in ArcGIS (ESRI, 2011) for creating a hydrologically corrected (sink-filled) DEM and extracting the flow direction. Terrain analysis using a DEM (TauDEM; Tarboton, 2003), is used for computing slope averaged over a selected distance (*SLPD*) along the direction of flow. Figure 3-2 shows the flow chart of the KET algorithm that calculates *SLPD* for different *d* values from

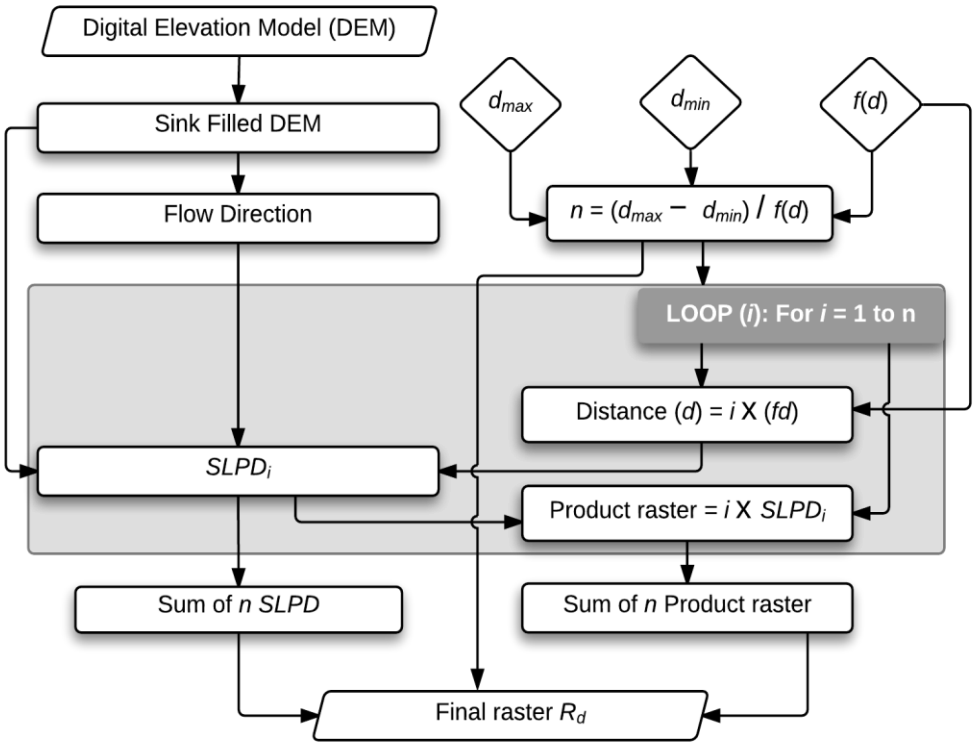

Figure 3-2: Flow chart of the algorithm used for Knickzone Extraction Tool (KET). The mathematical expression of R_d is explained in Equation 6.

d_{min} to d_{max} (the range of the gradient analysis) and represents the data as raster layers. The *SLPD* raster layers are used in the following equation for the calculation of R_d as a negative product of the regression coefficient signifying the decrease in gradient.

$$R_d = - \{n \sum x_i \, SLPD_i - \sum x_i \sum SLPD_i / n \sum x_i^2 - (\sum x_i)^2\} \qquad \text{Equation (6),}$$

where $n = (d_{max} - d_{min}) / f(d)$, $x_i = i \times f(d)$ n, and $SLPD_i$ is the i-th *SLPD* with $f(d)$ being a function of d that expresses the change in the multi-scale measurement distance from x_i to x_{i+1}. While Equation 4 provides numerical values of R_d for the downstream river gradient over a larger distance using elevation values, Equation 6 represents this value by averaging slope over marginal distances, resulting in raster layers. This raster-based approach that provides a regional raster layer of R_d values is advantageous compared to the manual calculation of R_d within individual river profiles. Using a threshold of R_d for extracting knickzones, KET identifies knickzones along with their height, length, distance from the stream top, and distance from the river mouth like SAKE.

3.3. Application of the knickzone extraction methods

The four knickzone extraction methods described in Section 3.1 and 3.2 were applied to the case study areas (c.f. Chapter 2) to obtain knickzone distribution maps. Knickzones with a length > 30 m and height ≥ 15 m were identified as well-defined knickzones. The range of stream length for gradient analysis using SAKE and KET (d_{min} to d_{max}) is 30 to 1500 m based on the spatial resolution of the DEM and varies with a step of 30 m. The height threshold of ≥ 15 m reflects the vertical accuracy of the DEM (originally prepared using topo-map contours with 10 m intervals) and the existence of small check dams that are not included in the dam data.

To extract knickzones with the SPT method, a concavity index (θ) for all the bedrock reaches is required (Equation 1). The calculated concavity index of 0.5 is used. Similarly, for GKF a mean curvature value is required and was calculated to be −0.49. A curvature threshold of −4 was used for this study because a threshold of −5 led to under-extraction of knickzones. This is because the calculated value of channel curvature (θ) from the head to the watershed outlet, along its longitudinal profile is −4 or −5 for the entire length of the channel. But a difference in gradient produces very different channel forms that influence the local curvature values. Underestimates of knickzones might occur because the same curvature values (here −5) can exist for bedrock rivers having different gradients.

The general properties of knickzones, such as their frequency (the total number of knickzones divided by the total length of bedrock reaches), density (the total length of knickzones divided by the total length of bedrock reaches), and forms including the average height, length and gradient (height divided by length) were calculated for knickzones using the four methods. Although the original version of GKF only provides concavity values of knickzones, we also extracted the height, length, and gradient properties.

Note that knickpoints from SPT are point data (knickpoints) along the river profile. As such, knickzone form characteristics like height, length, and gradient are not available. Characteristics like distance of the knickpoints from the river head and the watershed outlet were calculated from vector data of bedrock rivers because SPT does not provide them automatically. Alternatively, k_s from SPT indicates the scaling between drainage area and channel slope and the parameters of the Flint's Law (Equation 1) morphological characteristics of the river profiles. Similarly, morphological indices like mean concavity from GKF and R_d values from SAKE and KET were obtained for each knickzone. Trial runs were conducted with SAKE and KET (using a 64-bit operating system with a processing speed of 3.40 GHz and a

16 Gb RAM) to compare the time required for extracting knickzones using each method (details of which are mentioned in Section 4.1).

Sections 3.4 and 3.5 have been removed for future publication.

4. Analyses of Knickzones – Distribution, Properties and Form

The results from the comparative analyses of the new and existing methods of knickzone extraction (Chapter 3, Section 3.1 and 3.2) in the case study area of Gifu, and those from Kii have been grouped into three sub-sections: the distribution and basic properties of identified knickzones (Section 4.1), their abundance and morphometric properties (Section 4.2), and knickzone properties for different rock types (Section 4.3). The results of knickzones are identified using the SAKE method and KET, in the case study area of Kii has also been included in Sections 4.1.3 and 4.1.4. The properties of knickzones with morphometric characteristics and abundance (Section 4.2) consist of results from the different methods and they are compared using different DEM grid resolutions (Section 4.3), specifically for SAKE and KET, in Gifu and Kii respectively. The final section (Section 4.4) includes results concerning the formation of knickzones in two geologically different study areas of Gifu and Kii that are influenced by the environmental factors.

4.1. Distribution and basic properties

Distribution maps of the knickzones extracted based on the aforementioned methods depict high knickzone concentrations in the mountainous areas and southwestern slopes of Mount Ontake in the Gero watershed of Gifu (Figure 4-1). Whereas, in the Kumano watershed of Kii (Figures 4-2 and 4-3), the knickzones are concentrated in the central Yoshino highlands, along the upstream areas of the Kumano river to the east, and others scattered in the western highlands.

4.1.1. Knickzones from SPT

Using SPT, a total of 113 knickzones were extracted (Figure 4-1a). The frequency of the knickzones was 0.15 km^{-1}, with a mean upstream drainage area of 284.49 km^2 and a mean k_s value of 148.57. Individual extraction of 15 bedrock river longitudinal profiles and their knickzone extraction using the interactive profile and slope-area graphs in MATLAB and ArcGIS requires approximately one day. This time requirement, however, is dependent on the study area and the number of longitudinal profiles observed.

4.1.2. Knickzones from GKF

With the GKF tool, a total of 16 knickzones were extracted (Figure 4-1b). The mean concavity of all the bedrock streams was −0.49. The frequency of the knickzones was 0.02 km^{-1}, with a mean concavity of −7.93 indicating a high overall concavity. The percentage of knickzones in terms of length, i.e., density of knickzones, was very low (0.33%). The time required to run the GKF tool on a 10-m DEM was approximately one day.to run the GKF tool on a 10-m DEM was approximately one day.

4.1.3. Knickzones from the SAKE method

In Gifu, SAKE10 resulted in 141 knickzones (Figure 4-1c) with a frequency of 0.2 km^{-1}. The density of knickzones was 1.3%. The mean height of the knickzones was 27.47 m, the mean length was 69.68 m, the average gradient was 0.38 m m^{-1}, and mean R_d was 5.8×10^{-4} m^{-1}. SAKE50 extracted 58 knickzones (Figure 4-1d) for this study area with a frequency of 0.08 km^{-1}. The density of knickzones was 2.4% while the mean height, length, and gradient were 68.51 m, 311.72 m, and 1.73 m m^{-1}, respectively. The mean R_d was 3.58×10^{-5} m^{-1}. SAKE took less than 2 h to calculate R_d values for each longitudinal profile, but extracting the knickzones and their properties using spreadsheets took more than one day.

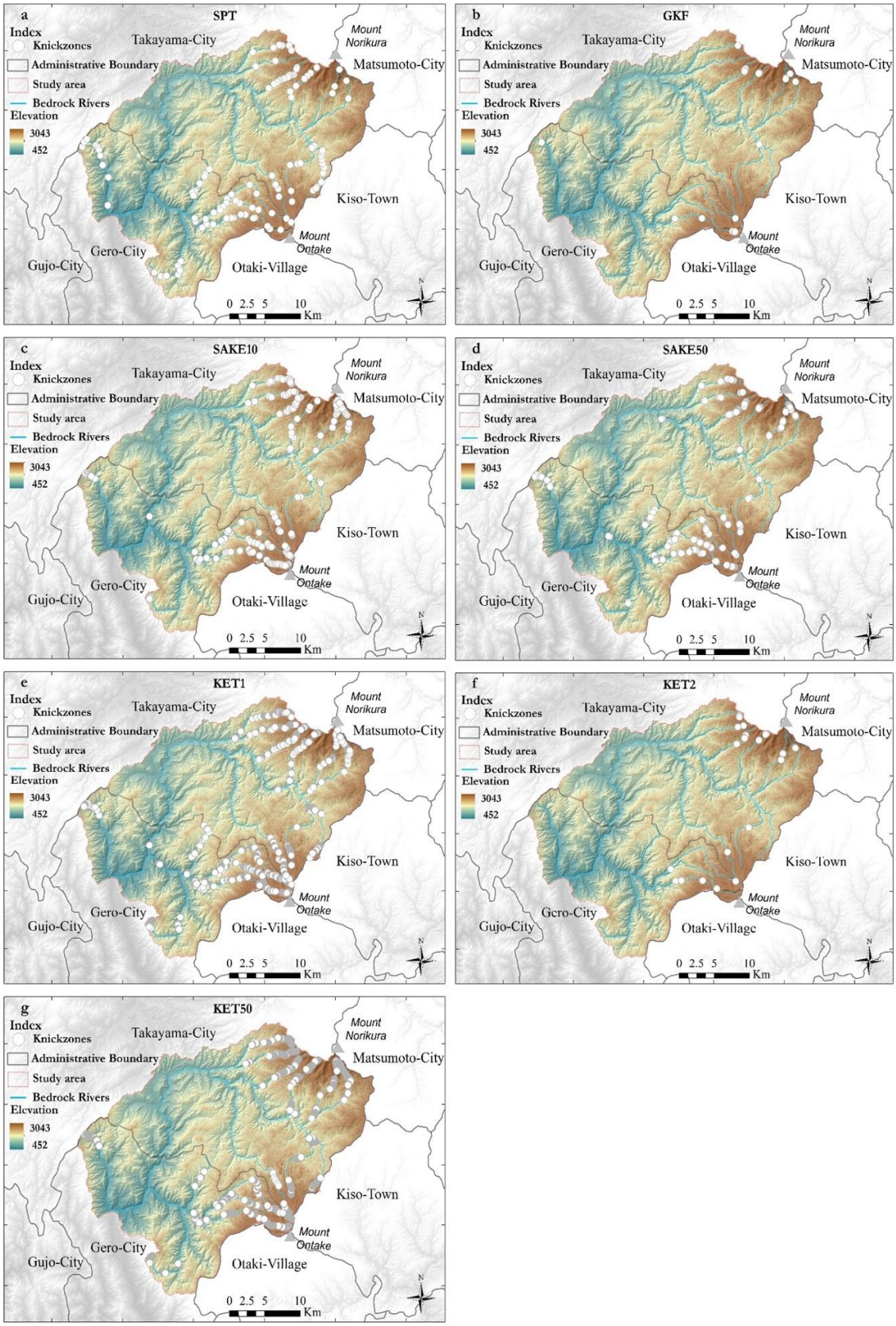

Figure 4-1: Distribution maps of knickzones in Gifu, extracted using the methods described in Section 3. a. STP; b. GKF; c. SAKE10; d. SAKE50; e. KET1; f. KET2, and g. KET50 (c.f. Section 4.1)

Whereas in Kii, SAKE10 resulted in 99 knickzones (Figure 4-2a) with a frequency of 0.03 km^{-1}. The density of knickzones was 0.37%. The mean height and length of the knickzones were 21.34 and 119.24 m respectively. While, the average gradient was 0.21 m m^{-1} and the mean R_d value was 5.18×10^{-4} m^{-1}. SAKE50 extracted 80 knickzones (Figure 4-2b) with a frequency of 0.03 km^{-1}. The density of knickzones was 1.22% while the mean height, length, and gradient were 53.59 m, 332 m, and 0.15 m m^{-1}, respectively. The mean R_d value was 6.08×10^{-2} m^{-1}. Since the total number of longitudinal profiles of bedrock rivers at Kii (34) was more than that in Gifu (15), calculating R_d values for each longitudinal profile took around 2 h, but extracting the knickzones and their properties using spreadsheets took more than two days.

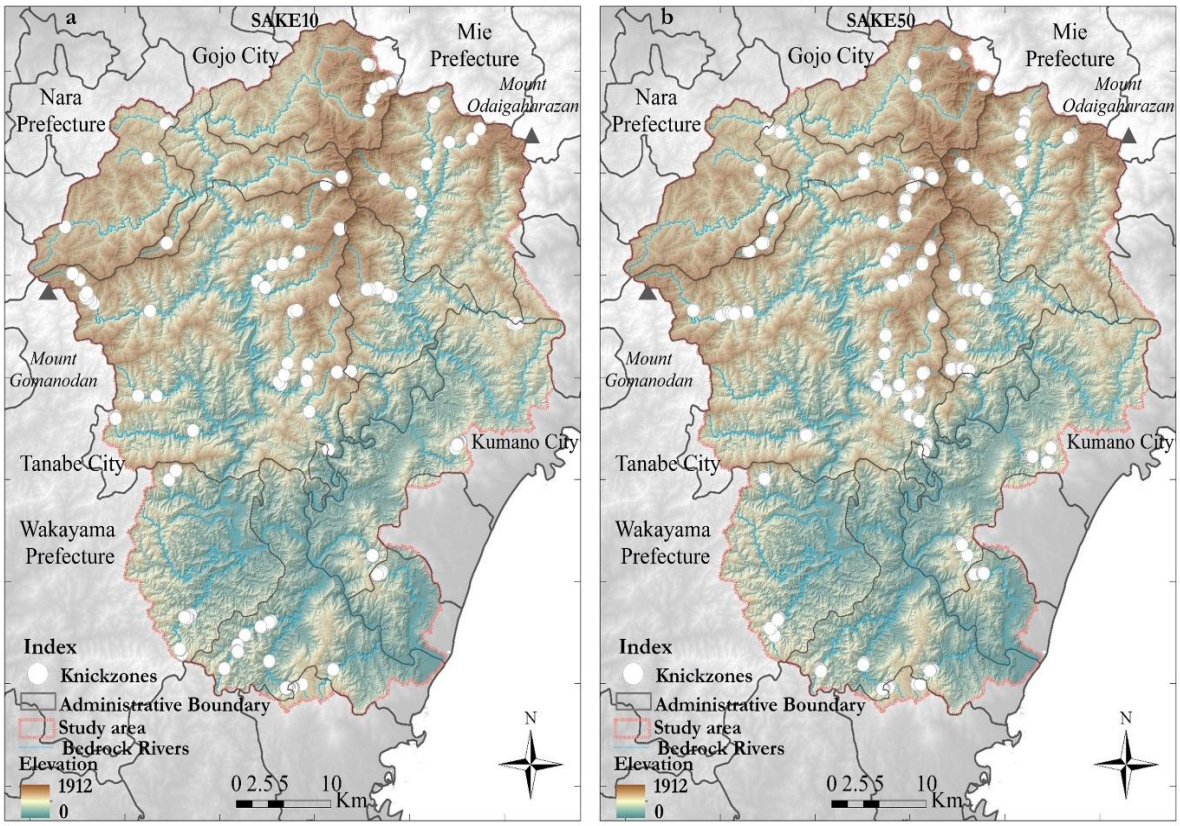

Figure 4-2: Distribution maps of knickzones in Kii, extracted using the SAKE method (a: 10-m DEM, b: 50-m DEM)

4.1.4. Knickzones from KET

In Gifu, KET1 resulted in a total of 189 knickzones (Figure 4-1e). The knickzone frequency is 0.25 km^{-1}. The density of knickzones was very high (8.14%) because each knickzone was long.

The mean height, length, and gradient of the knickzones were 33.83 m, 319.68 m, and 0.14 m m^{-1} respectively. The mean R_d was 6.8×10^{-4} m^{-1}. KET2 extracted 20 knickzones (Figure 4-1f). The knickzone frequency was 0.02 km^{-1} and the knickzone density was 0.32%. The mean value of knickzone length, height, and gradient were 48.43 m, 120 m, and 0.47 m m^{-1} respectively. The mean R_d was 2.71×10^{-4} m^{-1}. KET50 resulted in 111 knickzones (Figure 4-1g), with the knickzone frequency of 0.15 km^{-1}. The knickzone density is high (7.5%). The mean height, length, and gradient of the knickzones were 97.92 m, 501.22 m, and 0.16 m m^{-1}, respectively.

Table 1: General statistical properties of knickzone forms in Gifu

Statistics of form properties						
Methods	Properties	Units	Mean	Standard Deviation	Minimum	Maximum
GKF	Height	m	31.37	20.49	16.36	96.85
	Length	m	81.62	53.68	22.60	200.36
	Gradient	m m^{-1}	0.50	0.30	0.10	1.28
	Concavity		-7.93	1.44	-10.71	-5.99
SAKE10	Height	m	27.47	13.92	15.05	89.12
	Length	m	69.68	19.52	45.00	165.00
	Gradient	m m^{-1}	0.38	0.15	0.14	0.99
	Mean R_d	$\times10^{-4}$ m^{-1}	5.82	2.58	2.42	2.21×10^{-3}
KET1	Height	m	33.83	20.73	15.00	97.00
	Length	m	319.68	258.16	50.00	1770.00
	Gradient	m m^{-1}	0.14	0.08	0.02	0.5
	Mean R_d	$\times10^{-5}$ m^{-1}	-6.82	3.02	1.97×10^{-4}	-2.5
KET2	Height	m	48.43	21.94	20.13	106.51
	Length	m	120	59.03	40	240
	Gradient	m m^{-1}	0.47	0.26	0.2	1.15
	Mean R_d	$\times10^{-4}$ m^{-1}	-2.71	5.82	-4.28	-2.02
KET50	Height	m	97.92	130.43	5.54	952.56
	Length	m	501.22	450.69	60	2985
	Gradient	m m^{-1}	0.16	0.08	0.03	0.36
	Mean R_d	$\times10^{-5}$ m^{-1}	-2.78	9.61×10^{-6}	-6.22	-1.65
SAKE50	Height	m	68.51	64.61	11.10	355.10
	Length	m	311.72	137.91	160.00	880.00
	Gradient	m m^{-1}	1.73	1.29	0.92	7.86
	Mean R_d	$\times10^{-5}$ m^{-1}	3.58	2.00	1.63	10.81
NOTE: Knickpoints from STP are point data only, therefore form properties are not available.						

The mean R_d value was 5.6×10^{-3} m^{-1}. The average time required for trial runs of KET using a 50-m DEM in this study area was 15–20 minutes, while that for a 10-m DEM was 45–50 minutes. For comparison, the basic statistical values from the four methods with the results from different grid resolution DEMs and SAKE50 are shown in Table 1.

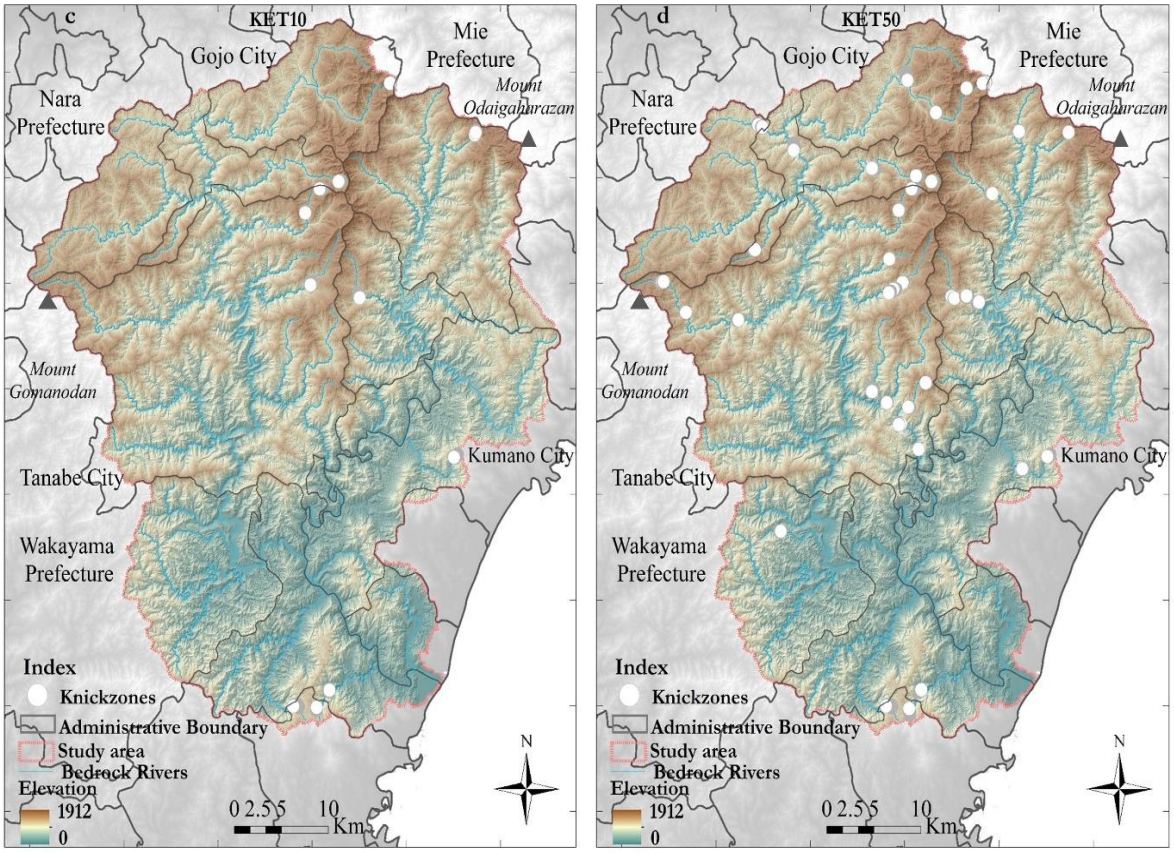

Figure 4-3: Distribution maps of knickzones in Kii, extracted using the KET (c: 10-m DEM, d: 50-m DEM)

In Kii, the KET10 resulted in 13 knickzones (Figure 4-3c) with a knickzone frequency of 0.004 km^{-1}. The density of knickzones was very low (0.14%) because the length of knickzone was low. The mean height, length, and gradient of the knickzones were 27.15 m, 334.62 m, and 0.20 m m^{-1} respectively. The mean R_d was 5.32×10^{-5} m^{-1}. KET50 resulted in 46 knickzones (Figure 4-3d), with the knickzone frequency of 0.01 km^{-1}. The knickzone density is 0.33%. The mean height, length, and gradient of the knickzones were 34.33 m, 227.50 m, and 0.39 m m^{-1}, respectively. The mean R_d was 1.83×10^{-6} m^{-1}. For comparison the basic statistical values from different grid resolution DEMs are shown in Table 2.

Table 2: General statistical properties of knickzone forms in Kii

Statistics of form properties						
Methods	Properties	Units	Mean	Standard Deviation	Minimum	Maximum
SAKE10	Height	m	21.34	6.33	15.11	54.81
	Length	m	119.24	52.02	45.00	270.00
	Gradient	m m^{-1}	0.21	0.10	0.07	0.59
	Mean R_d	$\times 10^{-4}$ m^{-1}	5.18	2.92	7.70×10^{-5}	1.3×10^{-3}
SAKE50	Height	m	53.59	42.52	15.10	216.60
	Length	m	332.00	132.95	80.00	720.00
	Gradient	m m^{-1}	0.15	0.09	0.05	0.43
	Mean R_d	$\times 10^{-2}$ m^{-1}	6.08	4.17	9.7010^{-3}	1.97×10^{-1}
KET10	Height	m	27.15	13.20	15.23	59.68
	Length	m	334.62	257.59	60.00	930.00
	Gradient	m m^{-1}	0.20	0.14	0.04	0.48
	Mean R_d	$\times 10^{-5}$ m^{-1}	5.32	2.24	1.8	1.06
KET50	Height	m	34.33	14.35	16.40	68.31
	Length	m	227.50	219.52	60.00	990.00
	Gradient	m m^{-1}	0.39	0.31	0.03	1.45
	Mean R_d	$\times 10^{-4}$ m^{-1}	1.83×10^{-6}	3.98×10^{-5}	-1.12	1.02

4.2. Knickzone morphometric properties and abundance

Analysis of the frequency of knickzones computed for each class of elevation, distance from the watershed outlet, drainage area and stream gradient for all the rivers (Figure 4-4) in Gifu reveals high frequency in two elevation zones: moderate elevations of 1600–2000 m and the other at higher elevations of 2200–2400 m (Figure 4-4a). The high elevation region lies within approximately 10–15 km of the river head. Knickzone frequency also shows local maxima at about 50–70 km distance from the watershed outlet (Figure 4-4b) for all the methods.

The frequency of knickzones for most methods reveals an abundance of knickzones in the smallest drainage area (10 km^2; Figure 4-4c), although SAKE10 gives the most abundant knickzones between 10–20 km^2, and KET2 does not give a clear trend because the number of knickzones is small. With an increase in stream gradient (Figure 4-4d), the SAKE10 result

shows increasing knickzone frequency until 0.24 m m^{-1} but a distinct decreasing trend in reaches steeper than 0.34 m m^{-1}. This trend is closely followed by KET2, with the highest frequency at 0.34 m m^{-1}.

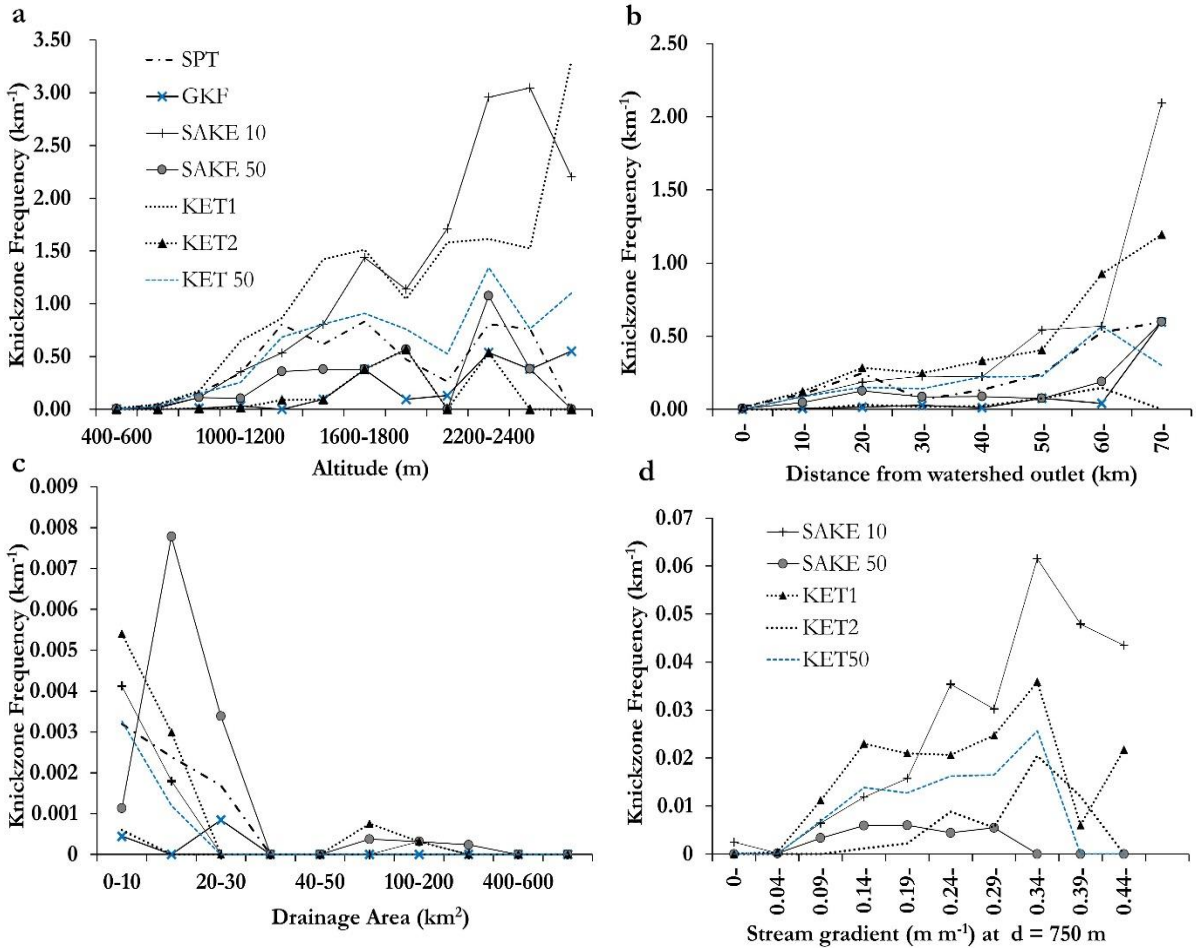

Figure 4-4: Knickzone frequency for different classes of a) altitude, b) distance from watershed outlet, c) drainage area, and d) stream gradient at d = 750 m for all bedrock rivers analyzed in Gifu.

Similarly analysis of frequency in Kii for each class of elevation, distance from the watershed outlet, drainage area and stream gradient for all the rivers (Figure 4-5) reveals high frequency of knickzones in two elevation zones: high elevations of 1200–1600 m and the other at low elevations of >1200 m (Figure 4-5a). The high elevation zones lie about 50–100 km of the river head with a local maxima at 120–150 km of the watershed outlet (Figure 4-5b). The frequency of knickzone reveals an abundance of knickzones in the smallest drainage areas (Figure 4-5c) mostly lying upstream in high elevation zones.

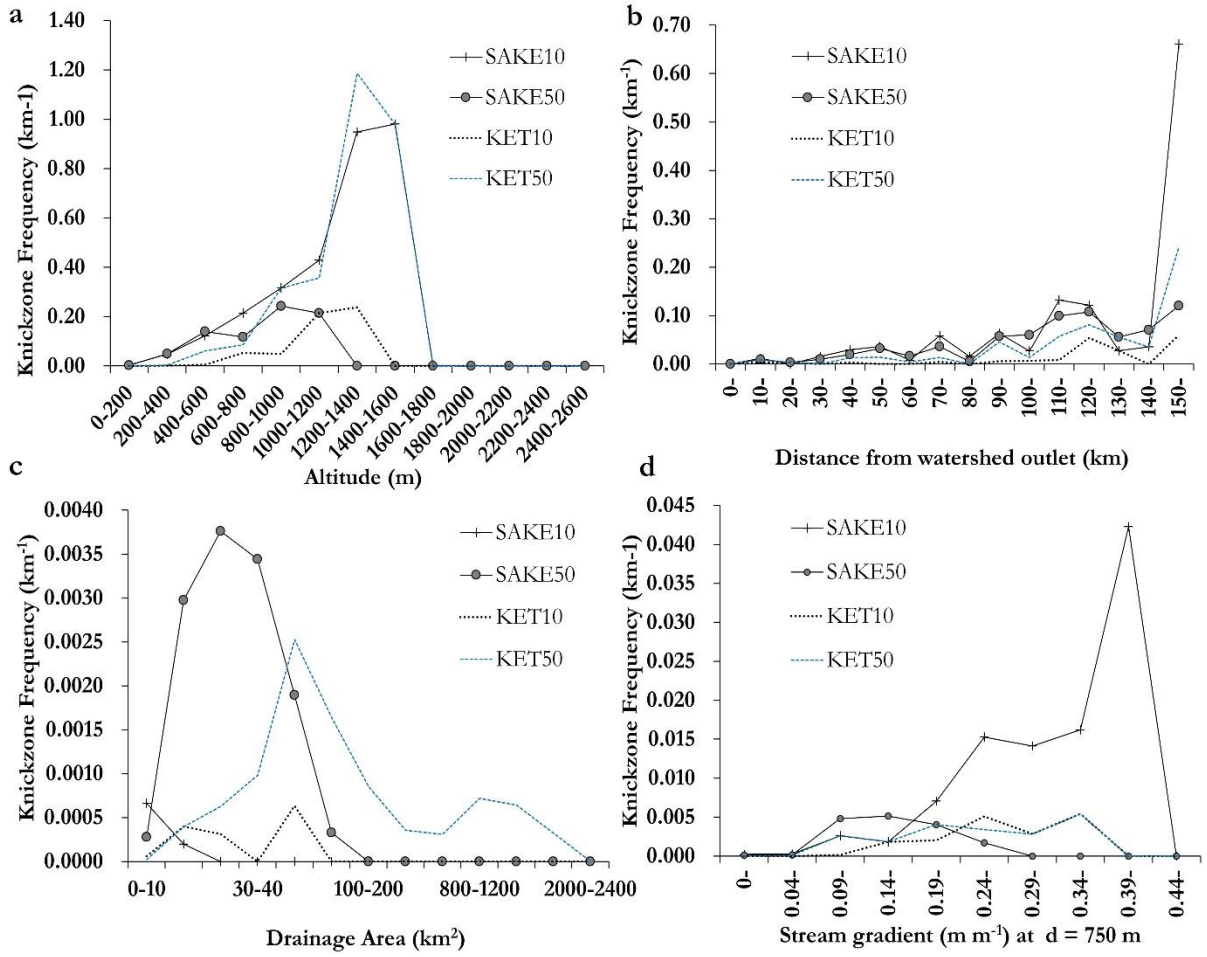

Figure 4-5: Knickzone frequency for different classes of a) altitude, b) distance from watershed outlet, c) drainage area, and d) stream gradient at d = 750 m for all bedrock rivers in Kii.

To further demonstrate the abundance of knickzones in each class of a locational parameter, knickzone frequency for altitude, distance to the river head, drainage area, and trend gradient of streams (Figure 4-6) were examined for different classes of height in Gifu to represent the form factor. Knickzones from KET1 reveal the frequency of occurrence with respect to form properties (Figure 4-4) more explicitly than the knickzones from KET2 as such the abundance of knickzones were determined using knickzones from KET1 (4-6, bottom), whereas knickzones from SAKE10 (4-6, top) were also used. Knickzone abundance information from SAKE50, KET2 and KET50 are available in Appendix I.

The height classes were determined using the knickzones at 25th, 50th and 70th percentiles (Figure 4-6, line graphs). The figures reveal that small knickzones (<18 m tall) are abundant in

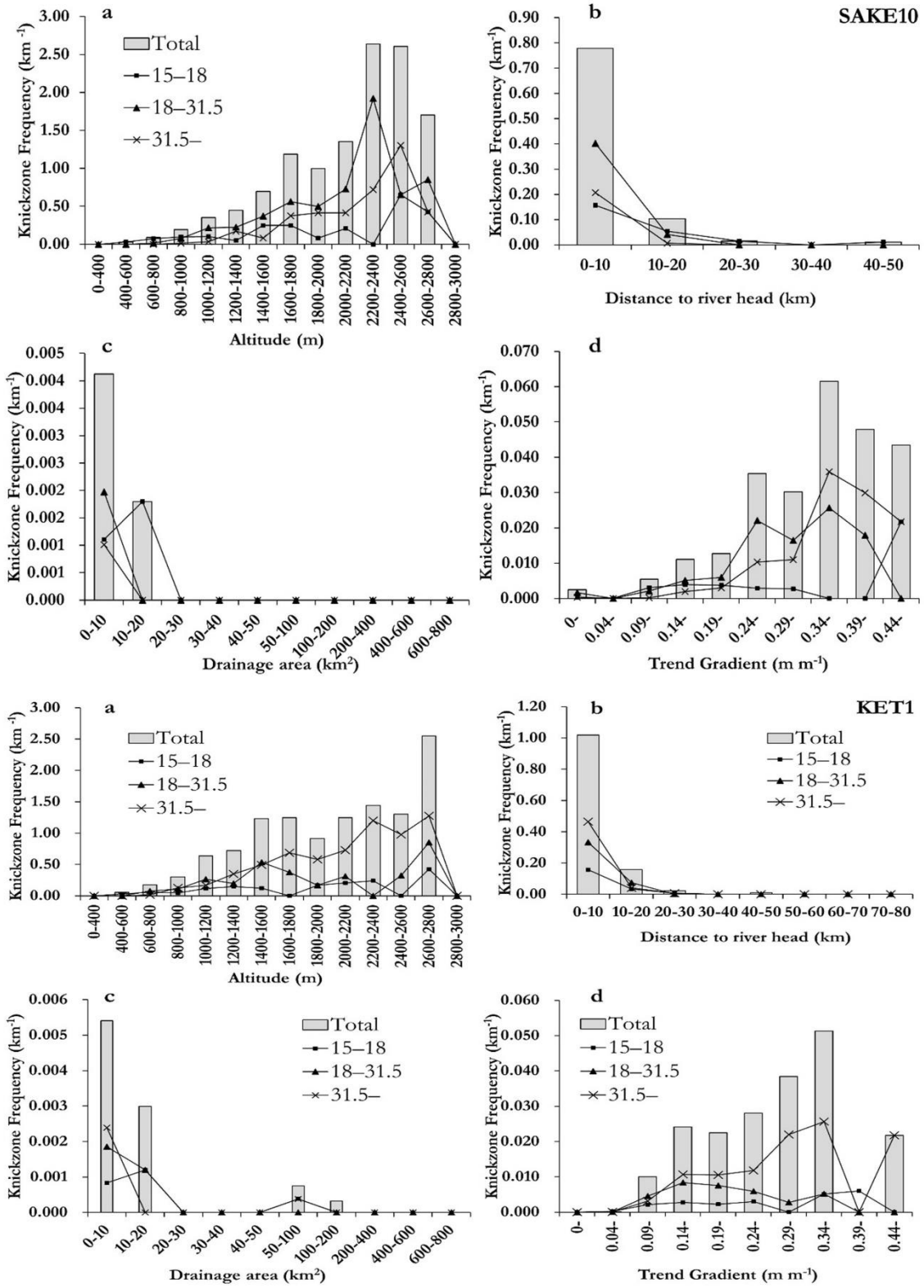

Figure 4-6: Knickzone frequency and locational factors for different height class for SAKE10 (top) and KET1 (bottom) in Gifu. a. altitude; b. distance to river head; c. drainage area; and d. trend gradient at d = 750 m. Lines show the frequency of knickzones for different height classes: 25th, 50th and 75th percentiles.

elevations of 2600–2800 m (Figure 4-6a, SAKE10) and also frequent between 2000–2400 m (Figure 4-6a, KET1). Extremely large knickzones (>31.5) are frequent in 2200–2400 m and 2400–2600 m, but above 2800 m, no large knickzones exist (Figure 4-6a, SAKE and KET1). Smaller and larger knickzones are abundant within 20–30 km from the riverhead (Figure 4-6b, SAKE10 and KET1) but the majority of them show peaks at <10 km from the river head. A similar trend exists with respect to drainage area (Figure 4-6c SAKE10 and KET1) where smaller drainages correspond to abundance of both the smaller and larger knickzones. High river gradients (0.34 m m^{-1}) tend to result in larger knickzones (>31.5 m) (Figure 4-6d).

The abundance of knickzones in each class of a locational parameter, knickzone frequency for altitude, distance to the river head, drainage area, and trend gradient of streams (Figure 4-7) were also examined for different classes of height in Kii to represent the form factor. Unlike Gifu, the abundance of small knickzones (15–18 m) in Kii are within 400–1000 m elevations. Large knickzones (>18 m) peak at 1200–1400 m and 1400–1600 m respectively (Figure 4-7a, SAKE10). KET10 values reveal a similar trend where large knickzones peak at 1000–1200 m and 1200–1400 m respectively (Figure 4-7a, KET10). Within 20–30 km distance to the river head (Figure 4-7c, SAKE10 and KET10) and at small drainage areas (about 20 km^2), both small and large knickzones are found in abundance. It must be noted here that very large knickzones (>31.5 m tall) are found in lower elevation zones of 1000–1200 m with the highest trend gradient of 0.34 m m^{-1} (Figure 4-7d, SAKE10), and this trend of stream gradient is more explicitly captured in KET10 (Figure 4-7d, KET10) with peaks at 0.24 m m^{-1}.

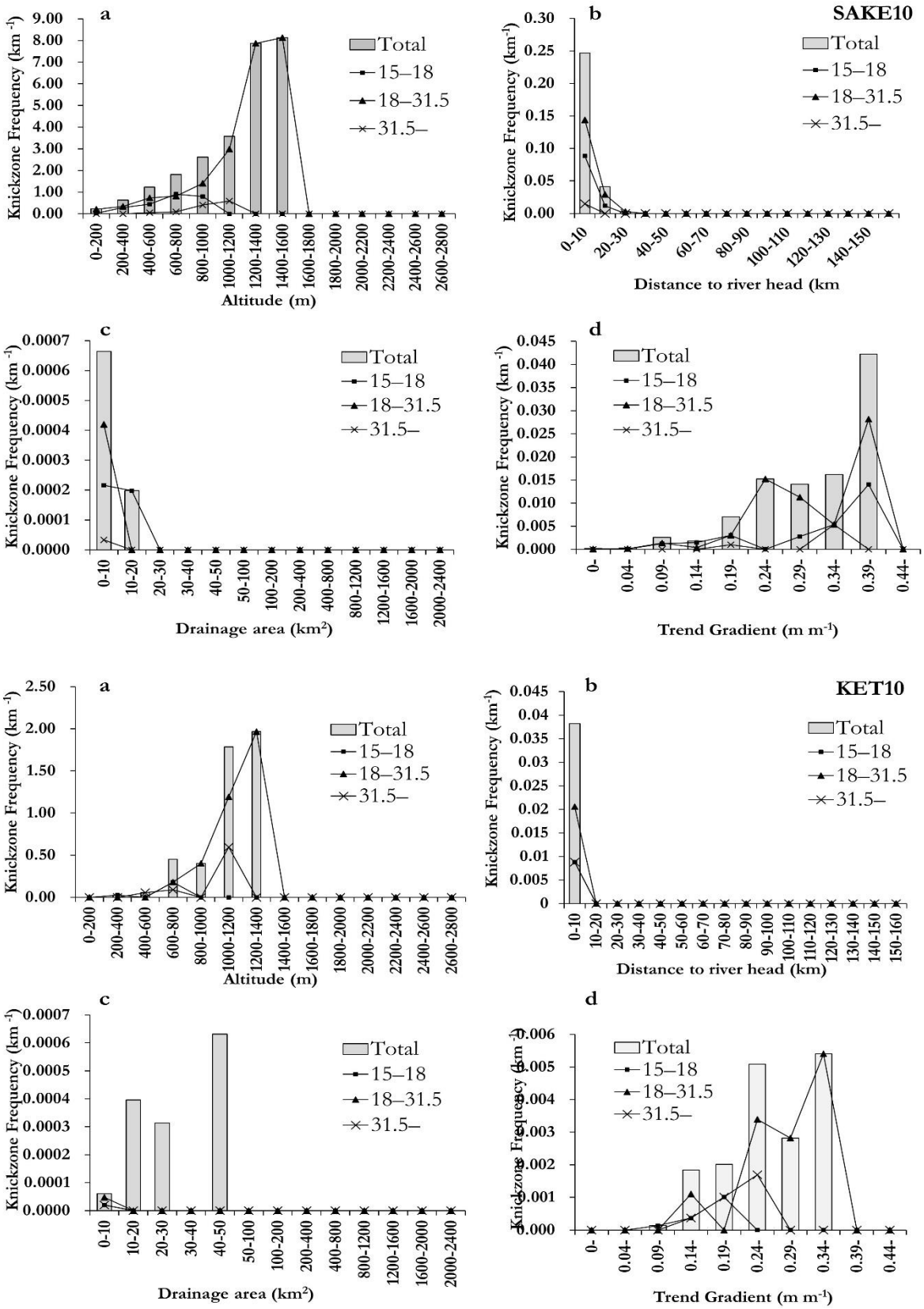

Figure 4-7: Knickzone frequency and locational factors for different height class for SAKE10 (top) and KET1 (bottom) in Kii. a. altitude; b. distance to river head; c. drainage area; and d. trend gradient at d = 750 m. Lines show the frequency of knickzones for different height classes: 25th, 50th and 75th percentiles.

4.3. Influence of DEM resolution and multi-scale gradients

The influence of DEM resolution and different scale range for stream gradients are also noticeable in Figures 4-4 and 4-5 for both Gifu and Kii respectively. In Gifu (Figure 4-4), the frequency of knickzones computed for elevation class (Figure 4-4a), distance from the watershed outlet (Figure 4-4b) and drainage area (Figure 4-4c) from the 50-m DEM show a similar trend to that from the 10-m DEM, except that the values are higher than those from a 10-m DEM. Knickzones from SAKE50 (Figure 4-4d) depict an increasing trend gradient at 0.14, 0.19, and 0.29 m m^{-1}, respectively. The results from KET1 are similar to those from SAKE10 and SAKE50. The same is true for KET50, which follows the same trend as KET1 and uses the same scale range for the stream gradient calculation despite different DEM resolutions. In Figure 4-4d, KET50 follows the same trend as SAKE50 at 0.19 and at 0.34 m m^{-1}, respectively, but both the results use a different scale ranges for the stream gradient calculation despite using the same DEM resolution.

In Kii (Figure 4-5), the influence of DEM grid resolution are very well captured in the frequency of knickzones computed for elevation class (Figure 4-5a), drainage area (Figure 4-5c) and the trend gradient of streams (Figure 4-5d). The frequency of knickzones from the 10-m DEM follow the trend as the 50-m DEM of elevation except that the values of elevation and drainage area are considerably higher. A similar trend is noticed in Figure 4-5d. A more detailed comparison of the influence of grid resolution on knickzone distribution and properties in Gifu and Kii are well depicted in Figure 4-8. A close observation reveals that in both the areas the frequency of knickzones with respect to altitude follows the same trend for different DEM grid resolutions (Figure 4-8a and b) but differs considerably with respect to drainage area (Figure 4-8g and h). Knickzone frequency at normalized upstream distance and the distance to the river head are high for SAKE10 in both Gifu and Kii. This could have been the case for KET10 too

if the number of knickzones identified for Kii were higher, though KET10 shows high values in Figure 4-8c.

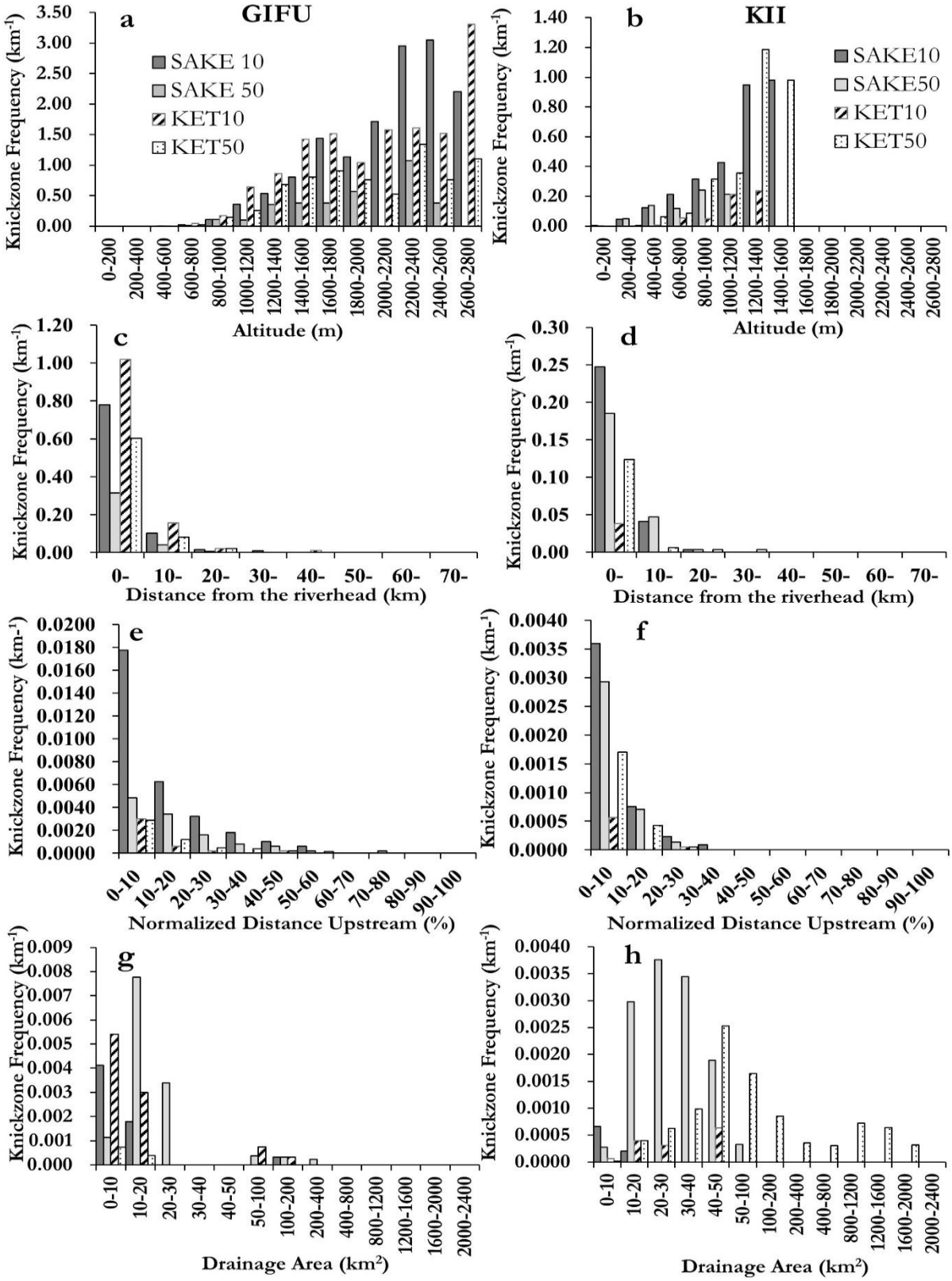

Figure 4-8: Comparison of the influence of 10-m and 50-m DEM grid resolutions on knickzone distribution and properties in Gifu and Kii using the SAKE method and KET

To further check the influence of DEM resolution, the gradient for d = 750 m derived from the SAKE method and KET were compared using knickzones along the longest river profile in the Gero watershed in Gifu (Figure 4-9).

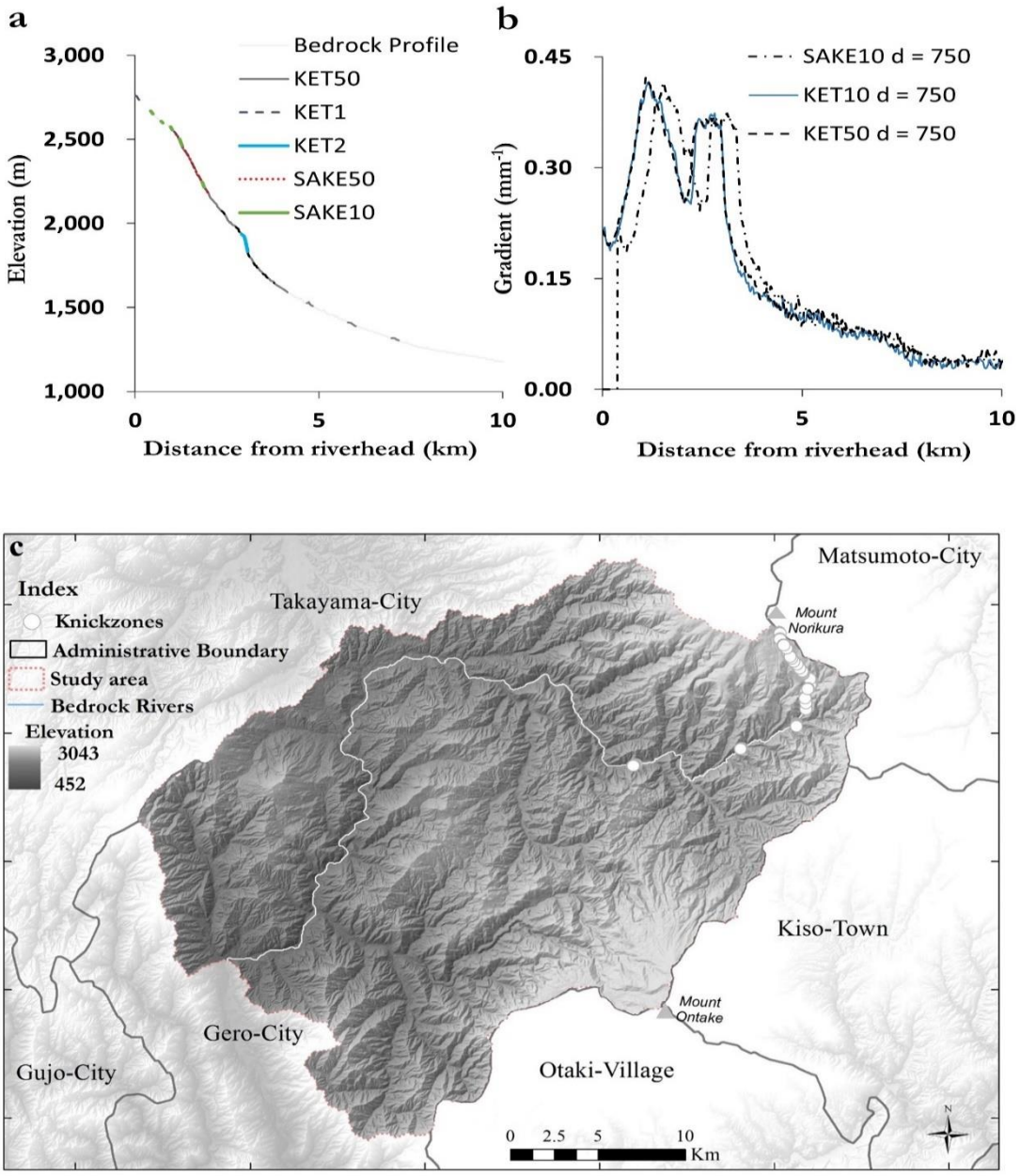

Figure 4-9: Comparison of results from SAKE and KET. a. Knickzone locations from the 50-m DEM (KET50 and SAKE50) and the 10-m DEM (KET1, KET2 and SAKE10) along a selected bedrock river. b. The gradient for d = 750 m derived from KET is almost the same for all grid resolutions. c. Selected profile along the study area. Note: Gradient information for SAKE50 was not available for d = 750 m because the scale range for trend gradient analysis used by Hayakawa and Oguchi (2009) is different from that used in this study.

Similarly, to check the influence of different input range scale on the R_d values using KET, knickzones were selected along a river profile with average R_d values for different input range scale (Figure 4-10) starting from 60 to 300 m and 60 to 540 m, respectively (Figure 4-10, top). The input scale range of 60 to 300 m was used to calculate the local threshold values for the SAKE method in both Gifu and in Kii. The input scale range of 30 to 1500 was used to calculate Equation 6 (c.f. Section 3.2), thereby generating the R_d raster map for both the study areas. This reveals that for different input range scales, their selection influences the average R_d values that are required to create thresholds for knickzone extraction, although the trend gradient values are similar (Figure 4-10, bottom).

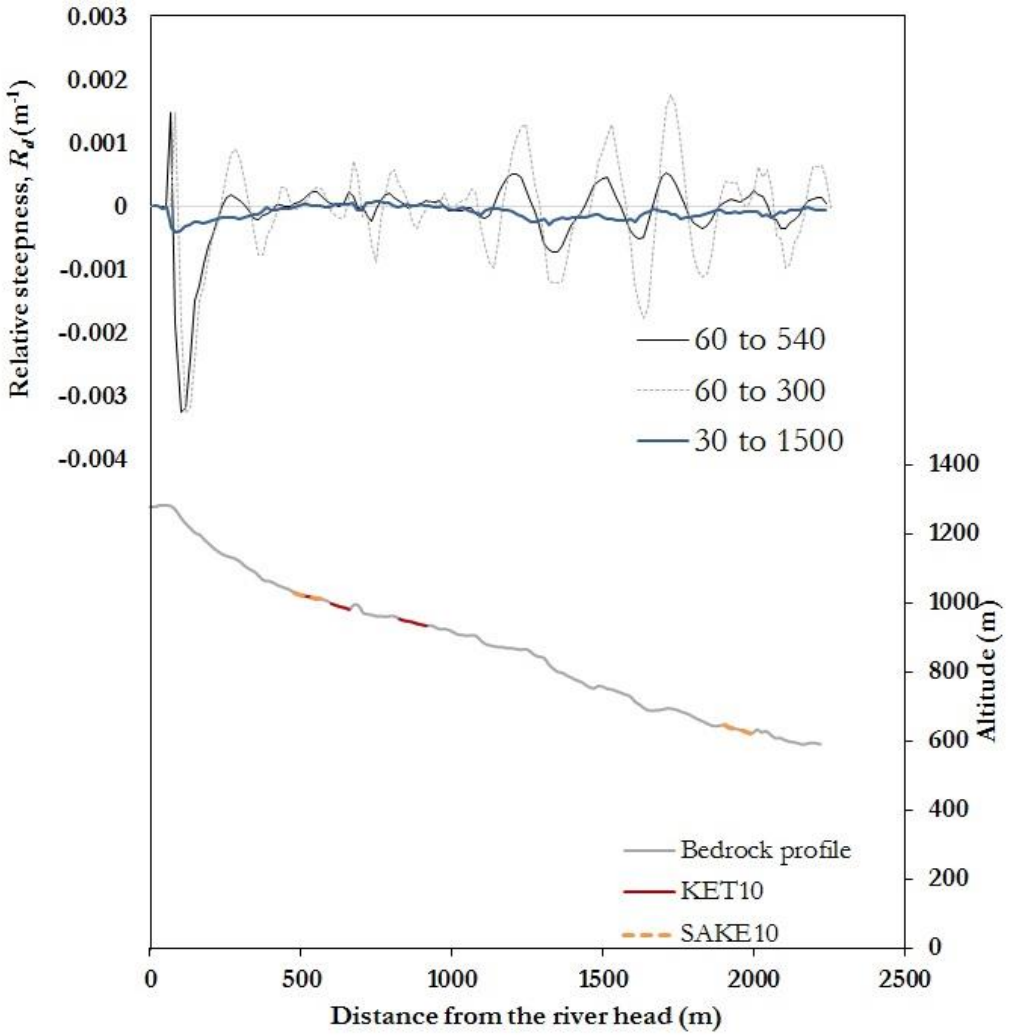

Figure 4-10: Top: Different input range scales 60 to 540 m, 60 to 300 m and 30 to 1500 m for calculating the average R_d. Bottom: Knickzones identified using KET and SAKE along a selected profile of a bedrock river in Kii.

Section 4.4 has been removed for future publication.

5. Quantitative Determination of Locational Accuracies of Knickzones

In an attempt to provide a quantitative locational accuracy of knickzones, results from the locational intersection of knickzones reveal the degree of intersection or overlap with respect to knickzones identified using each method in Gifu. In Kii, the probability of pixels provide quantitative estimates of locations identified as knickzones using different thresholds.

5.1. Intersection of knickzones in Gifu

Regarding the intersection of knickzones (Table 3), 36.28% of knickzones from KET1 were found within 90 m of knickzones extracted using the SAKE10 method. Interestingly, 76.25% of knickzones from SAKE10 were within 90 m of SPT knickzones, which was closely followed by 74.65% within 90 m of GKF knickzones; 59.32% of knickzones from SPT also intersected with KET1 at a distance of 90 m and the highest rate of intersection was 84.51% with respect to SAKE50. In contrast, the degree of intersection between KET1 and SAKE50 accounts for only 35.02% of knickzones. Intersection of knickzones of KET1 and GKF was 10.50%, while

Table 3: Proximity of knickzones from KET1, SAKE, GKF, and SPT

Degree of intersection in % AAA_BBB shows the percentage of 'BBB' knickzones within the buffer distance of 'AAA' knickzones						
Distance	SAKE10 _ KET1	KET1 _SAKE50	KET1 _SAKE10	KET1 _GKF	KET1 _SPT	SAKE50 _ KET1
15	15.84	72.18	67.63	40.13	41.53	10.93
30	20.26	75.00	71.88	66.91	53.39	22.55
45	24.75	78.52	73.75	72.74	54.24	30.32
60	29.04	80.63	74.38	73.42	55.08	31.83
75	33.02	82.04	75.38	74.04	57.63	33.51
90	36.28	84.51	76.25	74.65	59.32	35.02

those for SPT was 18.60%. At a distance of 45 m, 30.32 and 24.75% of knickzones from KET1 intersect with SAKE50 and SAKE10, respectively. In comparison, 80.00% and 86.54% of knickzones from KET2 intersect with knickzones from SAKE50 and SAKE10 at 45 m, respectively (Table 4).

At a distance of 90 m, 97.69% of knickzones from KET2 intersect knickzones from SAKE10, and 51.41% of knickzones from SAKE50 are within 90 m of the SAKE10 knickzones. Of the total knickzones extracted using SAKE10, 16.88% of the knickzones intersect with knickzones from KET2. Although the degree of intersection is highest for a distance of 90 m, considerably good results are also found at 45 m. The rates of increase of the percentage of intersection from 45 to 60 m, 60 to 75 m, and 75 to 90 m distance are approximately 1.15%, 0.39%, and 0.77%, respectively (Table 4, Column: SAKE50_KET2).

Table 4: Proximity of knickzones from KET2 and SAKE

Degree of intersection in % AAA_BBB shows the percentage of 'BBB' knickzones within the buffer distance of 'AAA' knickzones						
Distance	SAKE10 _ KET2	SAKE10 _SAKE50	KET2 _SAKE10	KET2 _SAKE50	SAKE50 _SAKE10	SAKE50 _ KET2
15	53.46	21.83	11.13	9.51	12.38	32.69
30	68.46	29.58	13.38	11.97	26.13	66.15
45	80.00	34.15	15.38	13.38	35.63	86.54
60	90.00	39.08	16.50	15.85	36.63	87.69
75	94.62	45.07	16.75	17.61	38.00	88.08
90	97.69	51.41	16.88	18.66	38.88	88.85

The degree of intersection between SPT and SAKE10 (Table 5) at 90 m distance is 33.05%, which is much lower than that for GKF (85.47%). This signifies that some knickzones from GKF, SAKE10, KET1, and KET2 intersect one another and also overlap knickzones from SAKE50 at different degrees of intersection. At a 15 m distance, SPT has very low values of intersection with all other methods, because the knickpoints are available as point data (refer to

Figure 4a), which reduces the possibility of intersection with knickzones extracted using other methods.

Table 5: Proximity of knickzones from GKF, SPT, and SAKE

Degree of intersection in % AAA_BBB shows the percentage of 'BBB' knickzones within the buffer distance of 'AAA' knickzones								
Distance	GKF_ SAKE10	GKF_ SAKE50	SAKE10 _GKF	SAKE50 _GKF	SPT_ SAKE10	SPT_ SAKE50	SAKE10 _SPT	SAKE50 _SPT
15	5.75	4.93	20.14	7.94	1.50	2.11	6.78	5.08
30	13.00	10.56	47.94	39.15	7.50	8.10	18.64	19.49
45	17.00	17.25	61.76	67.86	12.50	13.38	22.88	27.12
60	19.00	19.72	70.23	71.59	15.50	15.14	24.58	28.81
75	20.50	21.13	78.88	72.81	18.13	20.77	27.97	29.66
90	21.88	21.83	85.47	74.26	21.13	25.70	33.05	29.66

At a 15 m distance, the degree of intersection between KET50 and KET2 was 100%, whereas the degree of intersection between KET50 and KET1 was only 67.23%. This is because the knickzones from KET50 are longer than the well-defined knickzones with shorter lengths from KET1 and KET2. This is also the reason why the degree of intersection was highest with KET50 at a distance of 15 m for knickzones from all the methods (Table 6). Another reason is the small number of knickzones from KET2.

Table 6: Proximity of knickzones from KET50

Degree of intersection in % AAA_BBB shows the percentage of 'BBB' knickzones within the buffer distance of 'AAA' knickzones							
Distance	KET50 _SPT	KET50 _GKF	KET50 _SAKE10	KET50 _SAKE50	SAKE50 _KET50	KET1 _KET50	SAKE10 _KET50
15	31.86	48.20	64.50	72.18	10.32	63.51	15.53
30	19.47	36.88	3.50	3.17	10.45	3.77	5.32
45	2.65		2.88	2.82	8.25	3.09	5.13
60	0.88		1.88	1.41	1.70	2.72	5.68
75	2.65		1.63	3.17	1.83	2.36	5.00
90	3.54		1.13	1.41	1.81	1.94	4.14

However, the degree of intersection between SAKE50 and KET50 (10.32%) is much lower than that between SAKE10 and KET50 (15.53%). In the former case, the same threshold was used for the 50-m DEM, whereas the latter was used for the 10-m DEM with a different threshold for knickzone extraction. The intersection of knickzones KET50 and those from SPT and GKF was limited to distances of 15 and 30 m, and very few or no intersection was found at larger distances. This is because knickpoints from SPT are point data, whereas knickzones from GKF are small in number and located in the upstream areas.

Section 5.2 has been removed for future publication.

6. Discussion

The analytical results described in the previous chapters are discussed focussing on three distinct sections: 1) the use of the different methods of knickzone identification resulting in a regional scale distribution map emphasizing the need for a fast and automated approach; 2) the influence of DEM resolution and multi-scale stream gradients; and 3) the implication of the results with respect to the formation and development of knickzones at the Gero watershed in Gifu and the Kumano watershed in Kii. Additionally the locational accuracy of DEMs has also been assessed aiding the transferability of the KET in identifying knickzones.

6.1. Regional knickzone distribution with respect to different methods

The knickzone distribution maps and their morphological properties with respect to bedrock rivers, such as the normalized steepness index, curvature, and the relative steepness index, are not only useful for landscape evolution studies but are also important to studies that (1) rely upon tectonic and climatic signals stored in stream longitudinal profiles, (2) evaluate the parameters of stream incision, and (3) examine the effects of natural barriers upon aquatic biota. Though the SPT method is time-intensive, the resulting knickzones are used in tectonic uplift studies because the exponent of drainage-area and slope relationship includes parameters that represent uplift and erosion processes (Kirby and Whipple, 2001; Wobus et al., 2006a). The channel steepness (k_s), useful for tectonic geomorphic studies (Hoke et al., 2015; Sembroni et al., 2016) has been found to correlate with rates of rock uplift, exhumation, and stream incision (Andreani et al., 2014a,b). However, SPT is not particular useful for knickzone studies not directly related to tectonics. The GKF tool is still under development. Although it can be used

for analyzing and modeling gully head cut dynamics (Rengers and Tucker, 2014), it has not been fully implemented for extracting knickzones on a regional scale (Rengers, personal communication). Though SAKE calculates knickzone form parameters semi-automatically and has been used in applied studies (Yunus, 2015; Vatne et al., 2016; Yunus et al., 2016), using SAKE over large datasets will increase computational time because of its dependence on spreadsheet software for data analysis. Moreover, increasing use of high-resolution DEMs for geomorphological studies leads to increasing calculation times and computational bottlenecks (Liu et al., 2015). Thus, the development of a fast and automated process for regional knickzone mapping is therefore significant. KET is advantageous over all other methods because it is faster and more automated, as shown by the time required for runs using both the 50-m and 10-m DEMs to process large datasets as well as datasets of varying grid sizes and resolutions (Zahra, et al., in press). In recent years, increased availability of high-resolution airborne LiDAR DEMs may increase the possibilities of false detection of knickzones, regardless of the tool used. In this study KET actually yielded high R_d values for false knickzones especially at dam locations along the bedrock profile, which were manually eliminated. Although KET is more automated, careful consideration is needed in using it.

One of the drawbacks of KET is that, similar to the SAKE method, its initial input parameters, the range of the stream gradient calculation and the threshold of R_d, used for the determination of the knickzones are defined separately with a certain criteria. Because different thresholds for knickzone extraction result in different numbers of well-defined knickzones (Figures 4-1, 4-2 and 4-3), they influence the knickzone frequency values which are essential for comparison with morphometric characteristics. For example, in Figure 4-4, knickzones from KET1 reveal the frequency of occurrence with respect to form properties more explicitly than the knickzones from KET2 in Gifu. However, knickzones from SAKE10 and KET10 in Kii reveal the form properties more explicitly although the number of knickzones identified using KET10 are less

in number. Options for objective determination of thresholds will increase the usability of the KET for knickzones extraction and applied studies. The latest version of the KET with a tutorial and sample data are available at http://topography.csis.u-tokyo.ac.jp/resources/tools_ket/index.html. Any future updates of the tool and references to its applications in future studies will also be available at the above address.

6.2. Influence of DEM resolution and scale

The scale of the initial input parameters plays a significant role in determining the accurate location of knickzones along the bedrock rivers. The minimum distance for the calculation of G_d and R_d was 30 m for the 10-m DEM but 80 m for the 50-m DEM (Tables 1 and 2). If the threshold of R_d is within the input scale range for stream gradient calculation, the results are similar, even if different grid resolution DEMs are used (Figure 4-4d). Grid resolution, however, influences DEM derivative products such as slope and flow direction on a cell-by-cell basis (Hengl, 2006). In the case of knickzones extracted using the 50-m grid resolution, the aggregation of flow accumulation values have led to differences in the derivation of geomorphological properties; for example, concentrations of flow accumulation at each pixel (= drainage area) increases compared to knickzones for the 10-m grid resolution (Figure 4-4c). Advancements in mapping spatial patterns of streams, their morphometric parameters and related uncertainties (Lea and Legleitar, 2016; Tantasirin, et al., 2016) highlight the need to measure and analyse channel forms at different grid resolutions. In this study, the ability of the grid resolutions to capture the variability in the stream gradient (Figure 4-4d), an important aspect that varies spatially along the river, represents the influence of multi-resolution DEMs on knickzone extraction. Moreover, the R_d values derived from stream gradients that are used for thresholding and determining knickzones are also affected. This is because the suitability of the grid size for each type of terrain and the size of the area of interest influence the lengths of

the streamlines and channel slopes (Gallen et al., 2011; Buakhao and Kangrang, 2016), which subsequently alter not only the locations of knickzones but also their properties (Figures 4-6 and 4-8). This leads to uncertainty in the location of knickzones and their resulting distribution maps. This fact is illustrated in Figure 4-9, where knickzones extracted using all methods occur at similar locations in Gifu, along a selected bedrock river profile, exemplifying the importance of studying the influence of multi-resolution DEMs and the locational uncertainty of knickzone distribution in the future. Similarly, Figure 4-10 reveals how selection of different input scales for calculation of R_d has little implication on the identification of knickzones at locations along the bedrock rivers. The calculated threshold values differ with the change in the input scale range used for the calculation of R_d but the prominent knickzones extracted are along similar locations.

6.3. Influence of environmental factors on knickzone formation process

With respect to previous studies (Hayakawa and Oguchi, 2006, 2009), knickzones are found in upstream higher elevation zones of Japanese rivers suggesting the influence of fluvial hydraulics in the formation of knickzones. This is particularly true for Gifu where the abundance of knickzones in the upper reaches (Figure 4) is influenced by irregular relief and slope of the dominant volcanic rock. The Gero watershed in Gifu is part of the highest mountain ranges of the northern Japanese Alps and as such the bedrock rivers are very steep with high stream gradients in the upper reaches (Figure 4-4d). Studies in bedrock river profile suggest that hydraulic energy has the ability to shape bedrock morphologies when the rivers are sufficiently steep (Wohl, 1992; Baker and Kale, 1998). A wide range of stream gradients 0.19 to 0.39 m m^{-1} and more (Figure 4-4d) with knickzone frequency of 0.04 km^{-1} is characteristic of the highly erosive conditions. Abundance of knickzones in the bedrock rivers in Gifu can be attributed to this fact. However, the presence of deep seated gorges and canyons along with

knickzones with waterfalls in the dominant volcanic rocks in the Gero watershed can also be explained by the gradient irregularity (Figure 4-11 and 4-12) that is promoted by long-term exposure of steep channel slopes and coarse bedrock rivers (Wohl, 1992) to hydraulic action. The river gradient at d = 750 m, for volcanic, accretionary, sedimentary and plutonic rocks are 4.80×10^{-2}, 2.90×10^{-2}, 1.05×10^{-2} and 1.18×10^{-2} m m^{-1}, respectively. The plutonic and sedimentary rocks have high frequency owing to a short river stretch of 5 km in the former and a longer draining river of 230 km in the latter, but with fewer knickzones, indicating the effect of bedrock at least to some extent.

Some studies have stated that in steep reaches, hydraulic anomalies such as occurrence of supercritical flow along the reach can contribute to the formation of knickzones (Hayakawa, 2007). The positive correlation of precipitation to knickzone abundance also supports the fact that hydraulic forces are influenced by stream discharge though higher elevations together with steep slopes play a role in increased down-cutting of the channels. The large discharge in steep, bedrock channels might be non-uniform leading to hydraulic action where large amounts of energy are quickly dissipated (Kale et al., 1996). The positive correlation between relief and slope (Table 7) suggests that steep areas correspond to active denudation due to hydrological processes.

The presence of large knickzones (ca. 30 m) are restricted to upstream steep reaches, and smaller knickzones between 18 and 31 m and those <18 m are found in more gentle slopes (Figure 4-6). This suggests that the bedrock river profiles are not smooth graded profiles regardless of steepness and are suggestive of the non-equilibrium transient state of the river (Hayakawa and Oguchi, 2009) or the long profile disequilibria (Goldrick and Bishop, 2007).

In the Kii Peninsula, frequent typhoons and very highest frequencies of heavy rainfall (Saito and Matsuyama, 2012) contribute to abundance of knickzones in the upstream reaches. High stream gradients are found in the upstream high elevation reaches (Figure 4.13) underlain

mostly by accretionary rock complex that form the active denudation reaches in the Kumano basin. This is supported by the fact that the Cretaceous to Paleogene–lower Miocene Shimanto accretionary rock complex in the Kumano region is frequented by catastrophic landslides (Chigira, et al., 2013) and occurrence of knickzones (Hiraishi, et al., 2011). The high frequency of knickzones (0.01 to 0.045 km^{-1}) in high stream gradients ranging between 0.34 and 0.39 m m^{-1} in the accretionary rock complex (Figure 4.13d and 4.14 top d) explain the active action of the rivers.

Interestingly, knickzones frequency and density in Kii are high in plutonic rocks with the average river trend gradient of 0.085 m m^{-1}. Some studies in this region (Chigira, et al., 2013, 2015) have discussed river erosion with respect to deep-seated gravitational slope deformations and catastrophic landslides to conclude that the accretionary rock complex has paleosurface remnants at higher elevations (Figure 4.13 Inset) in the form of plutonic rocks. These paleosurface remnants have newly incised rivers in the central part of the Kii Mountains (Chigira, et al., 2015). These rivers with increased rates of river incision have widely developed knickzones. This explains the high knickzone frequency (Figure 4.15) in the plutonic rocks of the Kumano basin. The knickzones here are associated with canyons, waterfalls and often steep cliffs or gorges along the course of the river (Figures 5.3 and 5.4). In addition, the high frequency of knickzones in the volcanic rocks can also be associated with hydraulic action leading to the formation knickzones associated with steep canyons and gorges (Wohl et al., 1999) along the course of the river. This is evident by the presence of the Doryo-kyo (Kyo meaning Gorge in Japanese) that are distinct along the lower parts of the Kumano river.

As such, the Kumano basin consists of two sets of knickzone processes in the upstream and the downstream areas. The upstream areas are influenced by hydraulic action, while the downstream coastal area is more influenced by volcanic rocks similar as in the case with the Gero watershed in Gifu. It is difficult to make definitive, quantitative statements about the

processes by which rivers erode the bedrocks forming knickzone within a watershed. Even though both the watersheds are similar in average slope and shape, the trend gradients vary considerably (Figure 6.1). While river profiles are more complex with abundant knickzones in both the regions, evidences from the knickzone frequency of 0.2 km^{-1} in Gifu while that of 0.03 km^{-1} in Kii. This observation suggests that watersheds and river profiles should be analyzed independently to understand the nature of the fluvial landforms.

6.4. Accuracy of knickzone locations

This study attempts to quantify the accuracy of knickzone locations using the two different vector and raster based methods for both the study areas. The results look satisfactory and provide an idea of the degree of intersection of knickzones. Although they do not assure the correspondence to actual field locations of knickzones, the results can still be used as supporting information before field validation of knickzones. Knickzones with a degree of intersection higher than 80% at 90 m intersection distance in Gifu such as SAKE10 and KET2 (97.69%), KET1 and SAKE50 (84.51%), SAKE50 and KET2 (88.85%), and SAKE10 with GKF (85.47%) seem to provide approximate locations of well-defined knickzones. Note that SAKE10 suffers from over-extraction of knickzones it might influence the results. Moreover the extraction of only prominent knickzones in using KET might also influence the results. More detailed assessment is needed in future research.

The pixel based approach used in Kii is not free from ambiguity because the validated Google Earth images do not contain the information of the time when the photos were taken. Also most of the images are of waterfalls that might have been taken at or near tourist locations. In spite of these limitations, the probable locations of knickzones coinciding with SAKE50 (from Hayakaya and Oguchi, 2009) reveal approximate locations irrespective of DEM grid-resolution and the thresholds used.

7. Conclusion

This study applied the newly developed KET to central Japan and compared the results with other existing methods of knickzone extraction like STP, GKF and SAKE. The results indicate that KET is useful for extracting knickzones by detecting anomalies in the stream length gradient. KET performs well in detecting prominent knickzones in the upstream areas, although it is dependent on the applied threshold values, as is the case for the SAKE method. It is more automated and requires less time to run than the previous methods. Our analysis suggests that DEM resolutions do not significantly affect the detection of prominent knickzones, although they affect the values of some morphometric parameters.

Abundance of knickzones are mainly influenced by the irregular relief and slope characteristics that correlate well with hydraulic action in upstream reaches in Japan. Both in Gifu and in Kii, the formation of knickzones on the resistant volcanic rocks resistant represent typical examples of prolonged exposure (covering large timescales) of bedrocks to river incision and hydraulic actions.

This study also attempted to provide a quantitative assessment of accuracy of knickzones that supported the results from Hayakawa and Oguchi (2009) used for validation in the study. The method clarifies that knickzones coincide with similar locations though they might be identified using different resolution DEMs. They may not be at the exact location but along the same zone. Considering the complex formation of knickzones in the study areas the knickzones might not have migrated or changed positions.

Future research should include accuracy assessments based on field validated knickzone locations. Identification of knickzones using multi-scale values for generating streams

including the topographic base scale used for automatic generation of drainage networks should also be considered, to increase the applicability of the KET irrespective of scale of the drainage network. Additionally, considering the complex processes of knickzone formation in the Kii peninsula it is recommended to study sub-watersheds in accretionary rock complexes and volcanic rocks separately to understand the phenomena of knickzone formations.

Appendix

Abundance information for SAKE50, KET2 and KET50 for the Gero watershed in Gifu. a. altitude; b. distance from the river head; c. drainage area; d. trend gradient at d = 750 m.

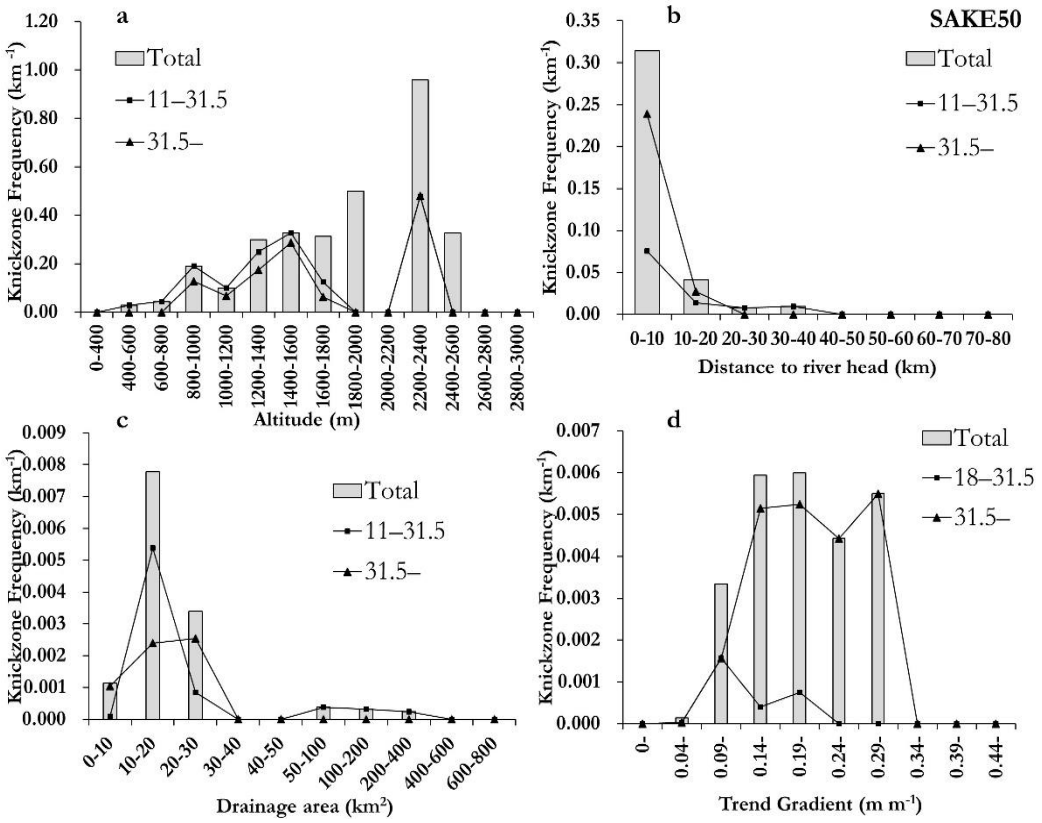

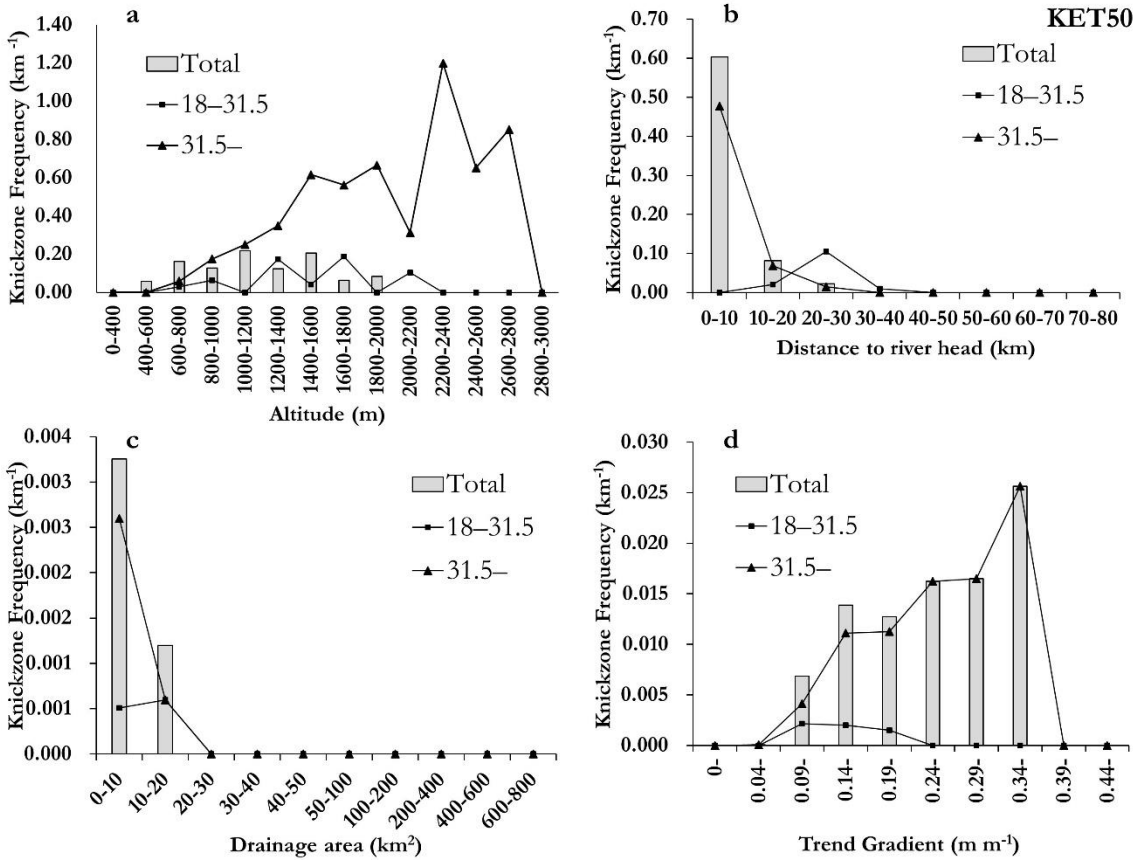
a
Total
18–31.5
31.5–
Knickzone Frequency (km -1)
Altitude (m)
b
KET50
Distance to river head (km)
c
Drainage area (km²)
d
Trend Gradient (m m-1)

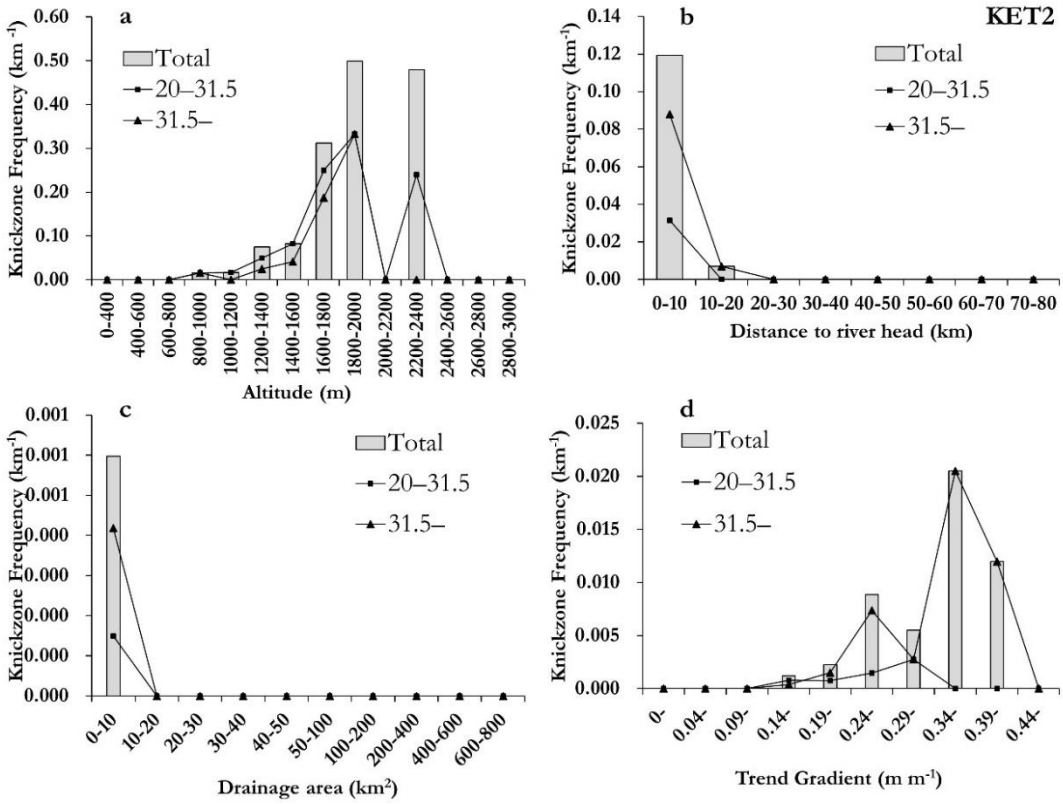
a
Total
20–31.5
31.5–
Knickzone Frequency (km -1)
Altitude (m)
b
KET2
Distance to river head (km)
c
Drainage area (km²)
d
Trend Gradient (m m-1)

Acknowledgements

You know the Greeks didn't write obituaries. They only asked one question after a man died: "Did he have passion?"

~~~ Serendipity (2001)

The very first line must have built a crease or two on your forehead. But put on your thinking caps, be patient and read along to find for yourself, how the road to PhD turned me into a movie-buff, a travel enthusiast, a souvenir hoarder, a camera geek, an Instagram-er, a web-content writer and maybe on the road to becoming the best chef in the world (that's exaggerated). I always thought of doing something out of the box and not stereotypical, this acknowledgement says it all. Since it is inspired from the movies I have watched to give me company while I worked sometimes all alone at my desk until wee hours in the morning. So read along.....

Patch Adams (1998), 'or as the poet Dante puts it: In the middle of the journey of my life, I found myself in a dark wood, for I had lost the right path. Eventually I would find the right path, but in the most unlikely place'. Indeed it turned out to be so after she vehemently extended her PhD and wanted to continue to stay in Japan against all odds. There was a brief phase when she did quote, '…..you have the ability to keep me from graduating. You can keep me (read as: keep me waiting) from getting the title and the white coat (read as: black and blue robes). But you can't control my spirit, gentlemen. You can't keep me from learning; you can't keep me from studying. So you have a choice: you can have me as a professional colleague, passionate, or you can have me as an outspoken outsider, still adamant.' (Hunter in Patch Adams, 1998). So that is that. She decided not to go away but to stay in Japan and face whatever came along. From being a girl who was 'too optimistic' to a girl 'with a character' she is grateful to her Supervisor, Professor Dr. Takashi Oguchi, who must have had a tough time dealing with her and yet continuously being an extreme gentleman by providing her with invaluable advice and

support, even though it was taxing on him at times. Thank you for sharing your knowledgeable and constructive insights, for cultivating her scientific thinking and polishing her academic writing skills. She still takes pride in telling everyone that hers was the only professor who made it for her Japanese language course commencement ceremony at the Hongo campus even though he has a very busy schedule. To her delight he was the chief speaker of the day too. Thank you for being there that day. She must have left Associate Professor Dr. Yuichi. S. Hayakawa completely bewildered with her teary eyed appearance one evening and innumerable emails. But she is grateful for having him around to help her with little snippets and comments that did make her think in newer directions. She confesses that she has been very aggressive often 'impolite' according to Japanese standards but she is indeed thankful to them for bearing with all her tantrums and weird working schedules. They may not even know that she had been fighting a battle with herself and that letting-her-be at times did help her to find her motivation and to get back to herself again. You have helped her to realize the fact that 'life will knock us down, but we can choose whether or not to stand back up' (Karate Kid, 2010) and as her Supervisor rightly puts it, 'persevere'. Thank You!

In the final days of her PhD life, she revealed an unknown side of her psyche. There was a hidden 'quasi-Jungian persona' that surfaced during her Milkha Singh*-like pursuit of a two-letter prefix to her name. The only thing that kept her chin up was hope. 'Hope is a dangerous thing, my friend, it can kill a man,' but don't worry because for her 'hope was a good thing, maybe the best of things, and no good thing ever dies' (Shawshank Redemption, 1994). Her best friend Chun Liang Lin aka Leo, a Taiwanese by origin and a Physicist by profession kept that hope alive in her, constantly motivating and standing by her side even for the silliest of reasons. But there were others to name a few; a simple Cambodian girl, Dr. Ches Sophy; Greek-goddess Christina Anagnostopoulou; Pinay (read Filipino) beer-buddy Tiffany Chua and Polish girl (pun intended) Dr. Ola Orman who were all ears to her hue and cry, apart from the

innumerable support from friends (Goutham, Mahendra, Shanthanu, Shashank, et al.) and seniors scattered all across the globe [worth mentioning are Dr. Salma Anwar *(Pakistan)*; Dr. Alka Singh (*Germany*), Dr. (to be) Ratna Sari Dewi (*Holland*), Fetty Febrianti (*Indonesia*) and Dr. Rashmi Kandwal (*USA*)]. She would also like to thank Dr. Ram Avatar, Dr. Wong Suh Song, Dr. Uttam Paudel and all the other lab members who helped her realize that, 'there are always possibilities' (Star Trek, 2009). Mrs. Ohnishi deserves special mention here. She not only listened to her but also brought a sense of calm and steadfastness midst all the chaos. Last but not the least Mrs. and Mr. Narita, a wonderful couple, who came forward to provide the warmth of a home with all the ease and amenities that helped her to stay focused on her thesis and strive for its completion. In addition, Yamamoto-San and her savoury delights at the Café on campus also deserve special mention. Thank you for all your kindness and support always.

Though she has specifically acknowledged many, yet there were some #AnonymousHeroes who brought a smile to her countenance, off and on. From the staff at the University entrance who bowed and uttered "Otsukaresamadesu" (meaning: keep up the hard work) be it morning, evening or night; to the ILO (International Liaison Office) staff, who sent reminder emails so that she could finish all administrative work well ahead of time. A big THANK YOU!

Ultimately what she concluded was that, 'you got a dream. You gotta protect it. People can't do something themselves, they wanna tell you, you can't do it. If you want something, go get it. Period,' (Pursuit of Happyness, 2006). Summing it up in the words of Kirk (Star Trek, 2009), "*It was the best of times; it was the worst of times…*"

Since, she is still learning to write grammatically correct sentences in academia after having read this, the word, '*Unremarkable* would be an upgrade for me, I assure you' (Seven Pounds, 2008).

Tuba Zahra

***Milkha Singh**, (born 1935), also known as The Flying Sikh, is a former Indian track and field sprinter. As of 2013, he is the only Indian male athlete to win an individual athletics gold medal at a Commonwealth Games. He represented India in the 1956 Summer Olympics in Melbourne, 1960 Summer Olympics in Rome and the 1964 Summer Olympics in **Tokyo**. He was awarded the Padma Shri, India's fourth-highest civilian honour, in recognition of his sporting achievements.

References

Ahnert. F., 1970. Functional relationships between denudation, relief and uplift in large mid-latitude drainage basins. American Journal of Science 268, 243–263.

Alexandrowicz, Z., 1994. Geologically controlled waterfall types in the Outer Carpathians. Geomorphology 9, 155–165. doi:10.1016/0169-555X(94)90073-6

Ambili, V., Narayana, A.C., 2014. Tectonic effects on the longitudinal profiles of the Chaliyar River and its tributaries, southwest India. Geomorphology 217, 37–47.

American Geological Institute, 1957. Glossary of Geology and Related Sciences.

Andreani, L., Gloaguen, R., Shahzad, F., 2014a. A new set of MATLAB functions (TecDEM toolbox) to analyze erosional stages in landscapes and base-level changes in river profiles. EGU General Assembly 2014.

Andreani, L., Stanek, K.P., Gloaguen, R., Krentz, O., Domínguez, L. G., 2014b. DEM-Based Analysis of Interactions between Tectonics and Landscapes in the Ore Mountains and Eger Rift (East Germany and NW Czech Republic). Remote Sensing 6(9), 7971–8001, doi:10.3390/rs6097971

Antón, L., De Vicente, G., Muñoz-Martín, A., Stokes, M., 2014. Using river long profiles and geomorphic indices to evaluate the geomorphological signature of continental scale drainage capture, Duero basin (NW Iberia). Geomorphology 206, 250–261, doi:10.1016/j.geomorph.2013.09.028

Anthony, D., Granger, D., 2007. An empirical stream power formulation for knickpoint retreat in Appalachian Plateau fluviokarst. Journal of Hydrology 343, 117–126.

Attal, M., Tucker, G., Whittaker, A., Cowie, P., Roberts, G., 2008. Modeling fluvial incision and transient landscape evolution: influence of dynamic channel adjustment. Journal of Geophysical Research 113. F03013, doi:10.1029/2007JF000893.

Bagnold, R.A., 1960. Some aspects of the shape of river meanders. Physiographic and hydraulic studies of rivers. Geological Survey Professional Paper 282-E.

Bagnold, R.A., 1977. Bed load transport by natural rivers. Water Resources Research 13, 303–312.

Baker, V.R., Kale, V.S., 1998. The role of extreme floods in shaping bedrock channels. In: Tinkler, K.J., Wohl, E.E., Rivers Over Rock: Fluvial Processes in Bedrock Channels Washington D.C., AGU Press. Geophysical Monograph Series 107, 153–165.

Beckers, A., Bovy, B., Hallot, E., Demoulin, A., 2014. Controls on knickpoint migration in a drainage network of the moderately uplifted Ardennes Plateau, Western Europe. Earth Surface Processes and Landforms 40, 357–374. DOI: 10.1002/esp.3638

Begin, Z.B., Meyer, D.F., Schumm, S.A., 1980. Knickpoint migration due to base level lowering: American Society of Civil Engineers Journal of the Waterway, Port, Coastal and Ocean Division 106, 369–388.

Begin, Z.B., Meyer, D.F., Schumm, S.A., 1981. Development of longitudinal profiles of alluvial channels in response to base-level lowering. Earth Surface Processes and Landforms, 6, 49–68.

Bennett, S.J., 1999. Effect of slope on the growth and migration of headcuts in rills. Geomorphology 30(3), 273–290.

Berlin, M.M., Anderson, R.S., 2007. Modeling of knickpoint retreat on the Roan Plateau, western Colorado. Journal of Geophysical Research 112, F03S06, doi:10.1029/2006JF000553

Bigi, A., Hasbargen, L.E., Montanari, A., Paola, C., 2006. Knickpoints and hillslope failures: Interactions in a steady-state experimental landscape. Geological Society of America Special Paper 398, 295–307.

Bilderback, E.L., Pettinga, J.R., Litchfield, N.J., Quigley, M., Marden, M., Roering, J.J., Palmer, A.S., 2014. Hillslope response to climate-modulated river incision in the Waipaoa catchment, East Coast North Island, New Zealand. GSA Bulletin 127(1/2), 131–148. doi: 10.1130/B31015.1

Bingner, R.L., Wells, R.R., Momm, H.G., Rigby, J.R., Theurer, F.D., 2016. Ephemeral gully channel width and erosion simulation technology. Natural Hazards 80, 1949–1966. DOI 10.1007/s11069-015-2053-7

Bishop, P., Goldrick, G., 1992. Morphology, processes and evolution of two waterfalls near Cowra, New South Wales. Australian Geographer 23, 116–121.

Bishop, P., Hoey, T.B., Jansen, J.D., Lexartzaartza, I., 2005. Knickpoint recession rate and catchment area: the case of uplifted rivers in eastern Scotland. Earth Surface Processes and Landforms 30, 767–778.

Bishop, P., 2007, Long-term landscape evolution: Linking tectonics and surface processes: Earth Surface Processes and Landforms 32(3), 329–365, doi: 10.1002/esp.1493.

Bressan, F., Papanicolaou, A., Thomas, J., Wilson, C., Elhakeem, M., 2013. Knickpoint migration and evolution in the Deep Loess Region of Western Iowa. In: World Environmental and Water Resources Congress, 1971–1980, doi:10.1061/9780784412947.193

Bressan, F., Papanicolaou, A., Abban, B., 2014. A model for knickpoint migration in first and second-order streams. Geophysical Research Letters 41, 4987–4996, doi:10.1002/2014GL060823.

Brocard, G.Y., Willenbring, J.K., Scatena, F.N., Johnson, A.H., 2015. Effects of a tectonically-triggered wave of incision on riverine exports and soil mineralogy in the Luquillo Mountains of Puerto Rico. Applied Geochemistry 63, 586–598. http://dx.doi.org/10.1016/j.apgeochem.2015.04.001

Botherton, M.A., 1982. Geology of Aggregate Resources in the Brazos and Colorado Floodplains of the Coastal Plains of Texas: Unpublished MS Thesis, Texas A&M University Graduate College, College Station, TX, December, 80.

Brice, J.C., 1964. Channel patterns and terraces of the Loup Rivers in Nebraska: U.S. Geol. Survey Prof. Paper, 422-D, 41.

Brush, L.M., Wolman, M.G., 1960. Knickpoint behavior in noncohesive material-Alaboratory study. Geological Society of America Bulletin 71, 59–73.

Buakhao, W., Kangrang, A., 2016. DEM Resolution Impact on the Estimation of the Physical Characteristics of Watersheds by Using SWAT. Advances in Civil Engineering, Article ID 8180158. http://dx.doi.org/10.1155/2016/8180158

Byun, J., Seong, Y.B., 2015. An algorithm to extract more accurate stream longitudinal profiles from unfilled DEMs. Geomorphology 242, 38–48. http://dx.doi.org/10.1016/j.geomorph.2015.03.015

Castillo, M., Bishop, P., Jansen, J.D., 2013. Knickpoint retreat and transient bedrock channel morphology triggers by base-level fall in small bedrock river catchments: The case of the Isle of Jura, Scotland. Geomorphology 180–181, 1–9.

Castillo-Rodríguez, M.E., 2011. Base-level Fall, Knickpoint Retreat and Transient Channel Morphology: The Case of Small Bedrock Rivers on Resistant Quartzites (Isle of Jura, Western Scotland). PhD thesis, University of Glasgow.

Chigira, M., Ching-Ying, T., Matsushi, Y., Hiraishi, N., Matsuzawa, M., 2013. Topographic precursors and geological structures of deep-seated catastrophic landslides caused by Typhoon Talas. Geomorphology 201, 479–493.

Chigira, M., Hiraishi, N., Ching-Ying, T., Matsushi, Y., 2015. Catastrophic landslides and their precursory deep-seated gravitational slope deformation induced by the river rejuvenation in the Kii Mountains, Central Japan. Engineering Geology for Society and Territory - Volume 2, 577-581 DOI: 10.1007/978-3-319-09057-3_95

Clemence, K.T., 1988. Influence of stratigraphy and structure on knickpoint erosion. Bulletin of the Association of Engineering Geologists 25, 11–15.

Crosby, B.T., Whipple, K.X., 2006. Knickpoint initiation and distribution within fluvial networks: 236 waterfalls in the Waipaoa River, North Island, New Zealand. Geomorphology 82, 16–38.

Davis, W.M., 1902. Base-level, grade, and peneplain. Journal of Geology 10, 77–111.

Davis, W.M., 1932. Piedmont benchlands and primarrumpfe. Geological Society of America Bulletin 43, 399–440.

Downs, P.W., Simon, A., 2001. Fluvial geomorphological analysis of the recruitment of large woody debris in the Yalobusha River network, Central Mississippi, USA. Geomorphology 37, 65–91, http://dx.doi.org/10.1016/S0169-555X(00)00063-5

ESRI, 2011 ArcGIS® Desktop (User's Manual).

Finnegan, N., Roe, G., Montgomery, D., Hallet, B., 2005. Controls on the channel width of rivers: Implications for modeling fluvial incision of bedrock. Geology 33(3), 229–232.

Flint JJ. 1974. Stream gradient as a function of order, magnitude, and discharge. Water Resources Research 10, 969–973.

Frankel, K., Pazzaglia, F., Vaughn, J., 2007. Knickpoint evolution in a vertically bedded surface, upstream-dipping terraces and Atlantic slope bedrock channels. Geological Society of America Bulletin 119(3-4), 476–486.

Fujieda, T., Kobayakawa, T., 1996. The knick points of the rivers on the border of Fuji and Ashitaka volcanoes. Numazu College of Technology Research Annual, 31, 97-108 (in Japanese).

Gallen, S.F., Wegmann, K.W., Frankel, K.L., Hughes, S., Lewis, R.Q., Lyons, N., et al., 2011. Hillslope response to knickpoint migration in the Southern Appalachians: implications for the evolution of post-orogenic landscapes. Earth Surface Processes and Landforms 36, 1254–1267.

Galve. J.P., Piacentini, D., Troiani, F., Della Seta, M., 2014. Stream length-gradient index mapping as a tool for landslides identification. In Mathematics of Planet Earth, Springer, 343–346.

García, A.F., Zhu, Z., Ku, T.L., Chadwick, O.A., Chacón Montero, J., 2004. An incision wave in the geologic record, Alpujarran Corridor, southern Spain (Almería). Geomorphology 60, 37–72.

Gardner, T.W., 1983. Experimental study of knickpoint and longitudinal profile evolution in cohesive, homogeneous material. Geological Society of America Bulletin. doi:10.1130/0016-7606(1983)94<664:ESOKAL>2.0.CO

Geological Survey of Japan, AIST (ed.), 2012. Seamless digital geological map of Japan 1:

200,000. Jul 3, 2012 version. Research Information Database DB084, Geological Survey of Japan, National Institute of Advanced Industrial Science and Technology.

Gilbert, G. K., 1877. Report on the geology of the Henry Mountains: U. S. Geol. Geog. Survey Rocky Mtn. Region, Rept., 160.

Goldrick, G., Bishop, P., 1995. Differentiating the roles of lithology and uplift in the steepening of bedrock river long profiles: An example from South-Eastern Australia. Journal of Geology 103, 227–231.

Goldrick, G., Bishop, P., 2007. Regional analysis of bedrock stream long profiles: evaluation of Hack's SL form, and formulation and assessment of an alternative (the DS form). Earth Surface Processes and Landforms 32, 649–671.

Goudie, A., 2004. Encyclopedia of Geomorphology, Taylor and Francis.

Grimaud, J.L., Paola, C., Voller, V., 2015. Experimental migration of knickpoints: influence of style of base-level fall and bed lithology. Earth Surface Dynamics Discussions 3, 773–805, doi:10.5194/esurfd-3-773-2015

Hack, J.T., 1957. Studies of longitudinal stream profiles in Virginia and Maryland. United States Geological Survey Professional Paper, 294-B.

Hack, J.T., 1973. Stream-profile analysis and stream-gradient index: U.S. Geological Survey Journal of Research 1, 421–429.

Hallet, B., Finnegan, N., Stewart, R.J., Montgomery, D.R., Anders, A., Zeitler, P., Koons, P., 2004. Self-organized balance between rapid erosion and uplift in the eastern Himalayan syntaxes. AGU Fall Meeting 2004, abstract T34B-07.

Hare, J.L., Ferguson, J.F., Aiken, C.L.V., Oldow, J.S., 2001. Quantitative characterization and elevation estimation of Lake Lahontan shoreline terraces from high-resolution digital elevation models. Journal of Geophysical Research 106, no. B11, 26761–26774.

Harvey, A.M., Wells, S.G., 1987. Response of Quaternary fluvial systems to differential epeirogenic uplift: Aguas and Feos river systems, southeast Spain. Geology, v. 15, 689–693.

Hasbargen, L. and Paola, C., 2000. Landscape instaibility in an experimental drainage basin. Geology 28, 1067–1070.

Hayakawa, Y., 2004. Form and Distribution of Fluvial Knickzones in Mountainous Watersheds: A GIS analysis for Kanto, Japan. Thesis for M.Sc., Department of Earth & Planetary Science, Graduate School of Science, the University of Tokyo, Japan.

Hayakawa, Y.S., 2007. Spatial Distribution and Formation of Fluvial Knickzones in Japanese Mountain Watersheds, PhD Dissertation, Department of Earth and Planetary Science, Graduate School of Science, the University of Tokyo.

Hayakawa, Y., Matsukura, Y., 2002. Rates of Waterfall Recession in Boso Peninsula, Japan. Thesis for B.Sc., College of Natural Science (Geoscience), First Cluster of Colleges, The University of Tsukuba.

Hayakawa, Y., Matsukura, Y., 2003a. Recession rates of waterfalls in Boso Peninsula, Japan, and a predictive equation. Earth Surface Processes and Landforms 28, 675–684.

Hayakawa, Y., Matsukura, Y. 2003b. Recession rate of Kegon Falls in Nikko, Tochigi Prefecture, Japanese Journal of Geography (Tokyo) 112, 521–530 (in Japanese with English abstract).

Hayakawa, Y.S., Oguchi, T., 2006. DEM-based identification of fluvial knickzones and its application to Japanese Mountain Rivers. Geomorphology 78, 90–106. doi:10.1016/j.geomorph.2006.01.018

Hayakawa, Y.S., Obanawa, H., Matsukura, Y., 2008. Post-volcanic erosion rates of Shomyo falls in Tateyama, Central Japan. Geografiska Annaler 90A, 65–74.

Hayakawa, Y.S., Oguchi, T., 2009. GIS analysis of fluvial knickzone distribution in Japanese mountain watersheds. Geomorphology 111, 27–37. doi:10.1016/j.geomorph.2007.11.016

Hayakawa, Y.S., Oguchi, T., 2013. Spatial correspondence of knickzones and stream confluences along bedrock rivers in Japan: implications for hydraulic formation of knickzones. Swedish Society for Anthropology and Geography. DOI:10.1111/geoa.12024

Haviv, I., Enzel, Y., Whipple, K., Zilberman, E., Stone, J., Matmon, A., Fifield, L., 2010. Evolution of vertical knickpoint (waterfalls) with resistant caprock: Insights from numerical modeling. Journal of Geophysical Research 115(F03028).

Van Heijst, M.W.I.M., Postma, G., 2001. Fluvial response to sea-level changes: a quantitative analogue, experimental approach. Basin Research 13, 269–292.

Heimsath, A.M., 2001. Chappel, J., Dietrich, W.E., Nishiizumi, K., Finkel, R,C., Late Quaternary erosion in southeastern Australia: a field example using cosmogenic nuclides. Quaternary International 83–85, 169–185

Hengl, T., 2006. Finding the right pixel size. Computers & Geosciences 32(9), 1283–1298. doi:10.1016/j.cageo.2005.11.008

Hill, J.S., Stewart, K.G., 2014. Automatic selection of knickpoints in longitudinal river profiles using open-source R script and a combination of normalized steepness, smoothed slope, and sum of the differences. 2014 GSA Annual Meeting (abstract only).

Hiraishi, N., Chigira, M., Matsushi, Y., 2011. Convex slope breaks in the Tenkawa District, Northern Kii Mountains. Annuals of Disaster Prevention Research Institute, Kyoto University, no. 56B. http://hdl.handle.net/2433/181495 (in Japanese with English abstract).

Hoke, G.D., Graber, N.R., Mescua, J.F., Giambiagi, L.B., Fitzgerald, P.G., Metcalf, J.R., 2015. Near pure surface uplift of Argentine Frontal Cordillera: insights from (U-Th)/He thermochronometry and geomorphic analysis. From: Sepu´ lveda, S. A., Giambiagi, L. B., Moreiras, S. M., Pinto, L., Tunik, M., Hoke, G. D. & Farı´as, M. (eds), Geodynamic Processes in the Andes of Central Chile and Argentina. Geological Society, London, Special Publications, 399, 383–399, http://dx.doi.org/10.1144/SP399.4

Holland, W., Pickup, G., 1976. Flume study of knickpoint development in stratified sediment. Geological Society of America Bulletin 87, 76–82.

Hopkins, M.C., Dawers, N.H., 2015. Changes in bedrock channel morphology driven by displacement rate increase during normal fault interaction and linkage. Basin Research 27, 43–59, doi: 10.1111/bre.12072

Howard, A.D., 1994. A detachment-limited model of drainage basin evolution. Water Resources Research 30(7), 2261–2285.

Howard, A.D., Dietrich, W.E., Seidl, M.A., 1994. Modeling fluvial erosion on regional to continental scales, Journal of Geophysical Research 99, no. B7, 13971–13986.

Ide, S., 2001. Complex source processes and the interaction of moderate earthquakes during the earthquake swarm in the Hida-Mountains, Japan, 1998. Tectonophysics 334(1), 35–54

Jansen, J.D., Fabel, D., Bishop, P., Xu, S., Schnabel, C., Codilean, A.T., 2011. Does decreasing paraglacial sediment supply slow knickpoint retreat? Geology 39, 543–546.

Japan Meteorological Agency (JMA), 2014. Precipitation data. http://www.data.jma.go.jp/obd/stats/etrn/index.php

Jones, O.T., 1924. The Upper Towy drainage system. Geological Society of London, Quarterly Journal 80, 568–609.

Jewell, P.W., 2016. Quantitative identification of erosional Lake Bonneville shorelines, Utah. Geomorphology 253, 135–145.

Kale, V.S., Baker, V.R., Mishra, S., 1996. Multi-channel patterns of bedrock rivers: An example from the central Narmada basin, India. Catena 26(1–2), 85–98. http://dx.doi.org/10.1016/0341-8162(95)00035-6

Katsube, K., Oguchi, T., 1999. Altitudinal changes in slope angle and profile curvature in the Japan Alps: A hypothesis regarding a characteristic slope angle. Geographical Review of Japan 72B, 63–72.

Keller, E. A., 1986. Investigation of active tectonics: use of surficial earth processes. In Panel on Active Tectonics. National Academy press: Washington, D. C.

Kirby, E., Whipple, K. X., Tang, W., Chen, Z., 2003. Distribution of active rock uplift along the eastern margin of the Tibetan Plateau: inferences from bedrock channel longitudinal long profiles. Journal of Geophysical Research 108, 2217.

Kirby, E., Whipple, K., 2000. Patterns of exhumation and rock uplift along the eastern margin of the Tibetan Plateau inferred from thermoschronology and bedrock river incision. Eos Transactions AGU, 81, Fall Meeting Supply Abstract T52F-03.

Kirby, E., Whipple, K., 2001. Quantifying differential rock-uplift rates via stream profile analysis. Geology 29, 415–418.

Kirby, E., Whipple, K., 2012. Expression of active tectonics in erosional landscapes. Journal of Structural Geology 44, 54–75.

Kooi, H., Beaumont, C., 1996. Large-scale geomorphology: Classical concepts reconciled and integrated with contemporary ideas via a surface process model. Journal of Geophysical Research 101(B2), 3361–3386.

Lave, J; Avouac, J.P., 2001. Fluvial incision and tectonic uplift across the Himalayas of central Nepal. Journal of Geophysical Research, v. 106, no. B11, 26561-26591.

Lague, D., 2014. The stream power river incision model: evidence, theory and beyond. Earth Surf. Process. Landforms 39, 38–61.

Lea, D.M., Legleiter, C.J., 2016. Mapping spatial patterns of stream power and channel change along a gravel-bed river in northern Yellowstone. Geomorphology 252, 66–79, doi:10.1016/j.geomorph.2015.05.033

Leopold, L., Bull, W., 1979. Base level, aggradation, and grade. Proceeding of the American Philosophical Society 123, 168–202.

Leopold, L., Wolman, G., Miller, J., 1964. Fluvial Processes in Geomorphology. Dover Publications, USA.

Lewis, W.V., 1945, Nick points and the curve of water erosion. Geological Magazine 82, 256–266.

Lin, Z., Oguchi, T., 2004. Analysis of stream-net in bare lands using high-resolution Digital Elevation Models. Transactions, Japanese Geomorphological Union 24, 348.

Liu, K., Tang, G., Jiang, L., Zhu, A.X., Yang, J., Song, X., 2015. Regional-scale calculation of the LS factor using parallel processing. Computers & Geosciences 78, 110–122. doi:10.1016/j.cageo.2015.02.001

Loget, N., van den Driesseche, J., 2009. Wave train model for knickpoint migration. Geomorphology 106(3–4), 376–382.

Lucien, M., Brush, Jr., Wolman, M.G., 1960. Knickpoint behavior in noncohesive material: A laboratory study. Bulletin of the Geological Society of America 71, 59–74.

Lyons, N.J., Mitasova, H., Wegmann, K.W., 2014. Improving mass-wasting inventories by incorporating debris flow topographic signatures. Landslides 11, 385–397, doi:10.1007/s10346-013-0398-0

Matthews, J.A., 2013. Encyclopedia of Environmental Change: Three Volume Set, 602–603.

Macar, P.F., 1934. Effects of cut-off meanders on the longitudinal profiles of rivers. Journal of Geology 42, 523–536.

Manville, V., Newton, E.H., White, J.D.L., 2005. Fluvial responses to volcanism: resedimentation of the 1800a Taupo ignimbrite eruption in the Rangitaiki River catchment, North Island, New Zealand. Geomorphology 65, 49–70.

McKeown, F., Jones-Cecil, M., Askew, B., McGrath, M., 1988. Analysis of stream-profile data and inferred tectonic activity, eastern Ozark Mountains Region. U.S. Geological Survey Bulletin 1807.

Merritts, D., Vincent, K.R., 1989. Geomorphic response of coastal streams to low, intermediate and high rates of uplift, Mendocino junction region, Northern California, Geological Society of America Bulletin 101, 1373–1388.

Merritts, D., Ellis, M., 1994. Introduction to special section on tectonics and topography. Journal of Geophysical Research 99, 12135–12141.

Miller, J.R., 1991. The influence of bedrock geology on knickpoint development and channel-bed degradation along downcutting streams in South-Central Indiana. The Journal of Geology 99, 591-605. doi:10.1086/629519.

Miller, S.R., Sak, P.B., Kirby, E., Bierman, P.R., 2013. Neogene rejuvenation of central Appalachian topography: Evidence for differential rock uplift from stream profiles and erosion rates. Earth and Planetary Science Letters 369–370, 1–12.

Ministry of Land, Infrastructure and Transport, 1988. Digital National Land Information: Climate Grid Data, G02-62M. http://nlftp.mlit.go.jp/ksj/.

Ministry of Land, Infrastructure and Transport, 1996. Digital National Land Information: Dam, W01-07P. http://nlftp.mlit.go.jp/ksj/.

Mino, Y., 1958. On the Kegon Water-Fall in Nikko, Tochigi Pref. Miscellany of Reports for Celebrating Professor H. Fujimoto's 60th Birthday. Kokusai–Bunken Press, Tokyo, 344–363 (in Japanese with English abstract).

Montgomery, D. R., Brandon, M., 2002. Topographic controls on erosion rates in tectonically active mountain ranges. Earth Planet. Sci.Lett. 201, 481–489.

Morisawa, M., 1960. Erosion rates on Hebgen Earthquake scarps, Montana (Abstract). Bulletin of the Geological Society of America, 1932.

National Institute of Industrial Science and Technology, 2012. Vector data of bedrock rivers in Japan. http://www.aist.go.jp/index_en.html

Niemann, J., Gasparini, N., Tucker, G., Bras, R., 2001. A quantitative evaluation of Playfair's Law and its use in testing long-term erosion models. Earth Surface Processes and Landforms 26, 1317–1332.

Ohmori, H, 1978. Relief structure of the Japanese mountains and their stages in geomorphic development. Bull. Dep. Geogr. Univ. Tokyo 10, 31–85.

Ohmori, H., 1991. Change in the mathematical function type describing the longitudinal profile of a river through an evolutionary process. Journal of Geology 99, 97–110.

Okunishi, K., 1974. Characteristic erosional processes in granitic drainage basins as found in Tanakami mountain range, Shiga Prefecture, Japan. Bulletin of Disaster Prevention Research Institute, Kyoto University 24, 233–261.

Parker, R.S., 1977. Experimental Study of Basin Evolution and Its Hydrologic Implications. Unpublished PhD dissertation, Colorado State University, Fort Collins, 331.

Parker, G., Muto, T., Akamatsu, Y., Dietrich, W.E., Lauer, J.W., 2008a, Unravelling the conundrum of river response to rising sea-level from laboratory to field. Part I: Laboratory experiments: Sedimentology 55, 1643–1655.

Parker, G., Muto, T., Akamatsu, Y., Dietrich, W.E., and Lauer, J.W., 2008b, Unravelling the conundrum of river response to rising sea-level from laboratory to field. Part II: The Fly-Stickland River system, Papua New Guinea. Sedimentology 55, 1657–1686.

Pavich, M.J., Jacobson, R.B., Newell, W.L., 1989. Geomorphology, Neotectonics, and Process Studies in the Rappahannock River Basin, Virginia, in IGC Field Trip T218 Guide: American Geophysical Union, 22.

Pazzaglia, F.J., Gardner, T.W., Merritts, D.J., 1998. Bedrock fluvial incision and longitudinal profile development over geologic time scales determined by fluvial terraces. Rivers Over Rock: Fluvial Processes in Bedrock Channels, Geophysical Monograph 1 07, American Geophysical Union.

Pederson, J.L., Tresslor, C., 2012. Colorado River long-profile metrics, knickzones and their meaning. Earth and Planetary Science Letters 345-348, 171–79.

Penck, W.O., 1925. Die piedmontflachen des sudlichen schwarswaldes. Gesellschaft fur Erdkunde, Berlin 1, 81–108.

Peters, J.J., 1978. Discharge and sand transport in the braided zone of the Zaire Estuary. Netherlands Journal of Sea Research 12, 273–292.

Philbrick, S.S., 1970. Horizontal configuration and the rate of erosion of Niagara Falls, Geological Society of America Bulletin 81, 3723-3732.

Phillips, J.D., McCormack, S., Duan, J., Russo, J.P., Schumacher, A.M., Tripathi, G.N., 2010. Origin and interpretation of knickpoints in the Big South Fork River basin, Kentucky–Tennessee. Geomorphology 114, 188–198.

Phillips, J., Lutz, J., 2008. Profile convexities in bedrock and alluvial streams. Geomorphology 102, 554–566.

Rengers, F., 2012. GIS-KnickFinder, https://github.com/csdms-contrib/gisknickfinder

Rengers, F., Tucker, G.E., 2014. Analysis and modeling of gully headcut dynamics, North American high plains. Journal of Geophysical Research-Eart 119, doi:10.1002/2013JF002962

Rosenbloom, N., Anderson, R., 1994. Hillslope and channel evolution in a marine terraced landscape, Santa Cruz, California. Journal of Geophysical Research 99(B7), 14013–14029.

Sakai, H., 1998. Causes of high-density waterfall distribution. Nature of Tokyo Metropolis, 24. Takao Natural Science Museum, Tokyo 1–21 (in Japanese).

Saito, H., Matsuyama, H., 2012. Catastrophic landslide disasters triggered by record-breaking rainfall in Japan: their accurate detection with Normalized Soil Wetness Index in the Kii Peninsula for the year 2011. SOLA 8, 081–084, doi:10.2151/sola.2012-021

Schumm, S.A., Hadley, R.F., 1957. Arroyos and the semiarid cycle of erosion. American Journal of Science 255, 161–174.

Schumm, S.A., Mosley, M.P., Weaver, W., 1987. Experimental Fluvial Geomorphology. John Wiley and Sons Inc., New York.

Seeber, L., Gornitz, V., 1983. River profiles along the Himalayan arc as indicators of active tectonics. Tectonophysics 92, 335– 367.

Seidl, M.A., 1993. Form and Process in Channel Incision of Bedrock. University of California at Berkeley Ph.D. thesis, Berkeley, California.

Seidl, M.A., Dietrich, W.E., 1992. The problem of channel erosion into bedrock. Functional Geomorphology; Landform Analysis and Models, Catena Supplement 23, 101–124.

Seidl, M., Dietrich, A., Kirchner, W., 1994. Longitudinal profile development into bedrock: An analysis of Hawaiian channels. Journal of Geology 102, 457–474.

Sembroni, A., Molin, P., Pazzaglia, F.J., Faccenna, C., Abebe, B., 2016. Evolution of continental-scale drainage in response to mantle dynamics and surface processes: An example from the Ethiopian Highlands. Geomorphology 261, 12–29, doi:10.1016/j.geomorph.2016.02.022

Siddique, S., Castaldini, D., Soldati, M., 2017. DEM-based drainage network analysis using steepness and Hack SL indices to identify areas of differential uplift in Emilia–Romagna Apennines, northern Italy. Arabian Journal of Geoscience 10, 3, DOI 10.1007/s12517-016-2795-x

Sinha, S., Parker, G., 1996. Causes of concavity in longitudinal profile of rivers. Water Resources Research 32(5), 1417–1428.

Sklar, L., Dietrich, W., 1998. River longitudinal profiles and bedrock incision models: Stream power and the influence of sediment supply., in Tinkler, K. and Wohl, E.E., eds., Rivers over Rock: Fluvial Processes in Bedrock Channels: Washington D.C., American Geophysical Union, Geophysical Monograph 107, 237–260.

Sklar, L. and Dietrich, W., 2004. A mechanistic model for river incision into bedrock by saltating bed load. Water Resources Research 40, W06301, doi:10.1029/2003WR002496.

Snow, S., Slingerland, R., 1987. Mathematical modeling of graded river profiles. Journal of Geology 95, 15–33.

Snyder, N., Whipple, K., Tucker, G., Merritts, D., 2000. Landscape response to tectonic forcing: DEM analysis of stream profiles in the Mendocino triple junction region, northern California: Geological Society of America Bulletin, v. 112, no. 8, 1250-1263.

Sohma, T., Kunugiza, K., 1993. The formation of the Hida nappe and the tectonics of Mesozoic sediments: the tectonic evolution of the Hida region, central Japan. Memoirs of the Geological Society of Japan 42, 1–20.

Stark, C.P., 2006. A self-regulating model of bedrock river channel geometry. Geophysical Research Letters 33, L04402.

Stein, O.R., Julien, P.Y., 1993. Criterion delineating the mode of headcut migration. Journal of Hydraulic Engineering 119(1), http://dx.doi.org/10.1061/(ASCE)0733-9429(1993)119:1(37)#sthash.4vtkKT8Q.dpuf

Stock, J.D., Montgomery, D.R., 1999. Geologic constraints on bedrock river incision using the stream power law. Journal of Geophysical Research 104(B3), 4983-4993.

Tantasirin, C., Nagai, M., Tipdecho, T., Tripathi, N.K., 2016. Reducing hillslope size in digital elevation models at various scales and the effects on slope gradient estimation. Geocarto International 31(2), 140–157, doi:10.1080/10106049.2015.1004133

Tarboton, D., Bras, R.L., Rodriguez-Iturbe, I., 1989. Scaling and elevation in river networks, Water Resources Research 25(9), 2037–2051.

Tarboton, D., 2003. Terrain analysis using digital elevation models in hydrology, in: 23rd ESRI International Users Conference. San Diego, California, 1–13

Tomkin, J., Brandon, M., Pazzaglia, F., Barbour, J., Willet, S., 2003. Quantitative testing of bedrock incision models for the Clearwater River, NW Washington State. Journal of Geophysical Research 106(B6 2308).

Tucker,G. E., Slingerland, R. L., 1997. Drainage basin response to climate change: Water Resources Research 33, 2031–2047.

Turowski, J., Hovius, N., Wilson, A., and Horng, M., 2008. Hydraulic geometry, river sediment and the definition of bedrock channles. Geomorphology 99, 26–38.

Van der Beek, P., Bishop, P., 2003. Cenozoic river profile development in the Uppler Lachlan catchment (SE Australia) as a test of quantitative fluvial incision models. Journal of Geophysical Research 108(B6).

Vatne, G., Irvine-Fynn, T.D.L., 2016. Morphological dynamics of englacial channel, Hydrol Earth System Science Discussions 12, 7615–7664, doi:10.5194/hessd-12-7615-2015

Von Engeln, O. D., 1940. A particular case of knickpunkte: Annals of the American Association of Geographers 30, 268-271.

Wakamatsu, T., Kubo, S., Matsuoka, M., Hasegawa, K., Sugiura, M., 2005. Japan Engineering Geomorphologic Classification Map. University of Tokyo Press, Tokyo.

Wei, Z., Bi, L., Xu, Y., He, H., 2015. Evaluating knickpoint recession along an active fault for paleoseismological analysis: The Hushan Piedmont, Eastern China. Geomorphology 235, 63–75. doi:10.1016/j.geomorph.2015.01.013.

Willenbring, J.K., Gasparini, N.M., Crosby, B.T., Brocard, G., 2013. What does a mean means? The temporal evolution of detrital cosmogenic denudation rates in transient landscapes. Geology 41, 1215–1218.

Willgoose, G., Bras, R., Rodriguez-Iturbe, I., 1991. A physical explanation of an observed link area-slope relationship. Water Resources Research 27(7), 1697–1702.

Whipple, K.X., 2004. Bedrock rivers and the geomorphology of active orogens. Annual Review of Earth and Planetary Sciences 32, 151-185. doi:10.1146/annurev.earth.32.101802.120356.

Whipple, K.X., Tucker, G.E., 1999. Dynamics of the stream-power river incision model: Implications for height limits of mountain ranges, landscape response timescales, and research needs. Journal of Geophysical Research 104, 17661. doi:10.1029/1999JB900120.

Whipple, K. X., Hancock, G. S., Anderson, R. S., 2000. River incision into bedrock: Mechanics and relative efficacy of plucking, abrasion and cavitation, Geological Society of America Bulletin 112 (3), 490–503.

Whipple, K.X., Wobus, C., Crosby, B., Kirby, E., Sheehan, D., 2007. New tools for quantitative geomorphology: extraction and interpretation of stream profiles from digital topographic data. In: Geological Society of America, Annual Meeting. NSF Geomorphology and Land Use Dynamics, Boulder Colorado.

Whitbread, K., Jansen, J., Bishop, P. Attal, M., 2015. Substrate, sediment, and slope controls on bedrock channel geometry in postglacial streams, Journal of Geophysical Research: Earth Surface 120, 779–798, doi:10.1002/2014JF003295.

Whittaker, A.C., 2012. How do landscapes record tectonics and climate? Lithosphere, v. 4, no. 2, 160–164. doi: 10.1130/RF.L003.1

Whittaker, A.C., Boulton, S.J., 2012. Tectonic and climatic controls on knickpoint retreat rates and landscape response times. Journal of Geophysical Research 117, F02024.

Wobus, C., Whipple, K.X., Kirby, E., Snyder, N., Johnson, J., Spyropolou, K., Crosby, B., and Sheehan, D., 2006a, Tectonics from topography: Procedures, promise, and pitfalls: Geological Society of America Special Papers 398, 55–74, doi: 10.1130/2006.2398 (04)

Wobus, C.W., Crosby, B.T., Whipple, K.X., 2006b. Hanging valleys in fluvial systems: Controls on occurrence and implications for landscape evolution. Journal of Geophysical Research: Earth Surface 111, 2003–2012.

Wobus, C.W., Kean, J.W., Tucker, G.E., Anderson, R.S., 2008. Modeling the evolution of channel shape: Balancing computational efficiency with hydraulic fidelity. Journal of Geophysical Research 113, F02004, doi:10.1029/2007JF000914

Wohl, E., 1992. Gradient irregularity in the Herbert Gorge of Northeastern Australia. Earth Surface Processes and Landforms 17, 69–84.

Wohl, E.E., Ikeda, H., 1998. Patterns of bedrock channel erosion on the Boso Peninsula, Japan. Journal of Geology 106(3), 331–346

Wohl, E., Achyuthan, H., 2002. Substrate Influences on Incised-Channel Morphology. Journal of Geology 110, 115–120.

Wohl, E.E., Thompson, D.M., Miller, A.J., 1999. Canyons with undulating walls. Geological Society of America Bulletin 111, 949–959.

Wolman, G., 1987. Sediment movement and knickpoint behaviour in a small piedmont drainage basin. Geografiska Annaler 69(1), 5–14.

Woodford, A.O., 1951. Stream gradients and Monterey Sea Valley: Geol. Soc. America Bull. 62, 799–852.

Yanites, B.J., Tucker, G.E., Mueller, K.J., Chen, Y.G., Wilcox, T., Huang, S.Y., Shi, K.W., 2010. Incision and channel morphology across active structures along the Peikang River, central Taiwan: Implications for the importance of channel width: Geological Society of America Bulletin 122, 1192–1208.

Yonekura, N., 1968. Geomorphic development and mode of crustal movement on the south coast of the Kii Peninsula, Southwestern Japan. Journal of Geography 77, 1 (in Japanese with English abstract).

Yunus, A. P., 2015 Morphometric Analysis of Drainage Basins in the Western Arabian Peninsula. Doctoral Thesis for the Department of Natural Environmental Studies. Graduate School of Frontier Science, the University of Tokyo.

Yunus, A. P., 2016. Geomorphic and lithologic control on bedrock channels in drainage basins of the Western Arabian Peninsula. Arabian Journal of Geoscience 9(133), doi:10.1007/s12517-015-2179-7

Yunus, A. P., Oguchi, T. and Hayakawa, Y.S., 2016. Remote identification of fluvial knickzones and their imprints on landscape morphology in the passive margins of Western Arabian Journal of Arid Environment 130, 14–29.

Zahra, T., Paudel, U., Hayakawa, Y.S., Oguchi, T., Knickzone Extraction Tool (KET) – A new ArcGIS toolset for automatic extraction of knickzones from a DEM based on multi-scale stream gradients (in press).

Zaprowski, B.J., Evenson, E.B., Pazzaglia, F.J., Epstein, J.B., 2001. Knickzone propagation in the Black Hills and northern High Plains: A different perspective on the late Cenozoic exhumation of the Laramide Rocky Mountains. Geology 29, 547–550.

Zeuner, F. E., 1945. The Pleistocene Period, 2nd ed., 447, Ray Society, Hutchinson, London.

Zeitler, P.K., Meltzer, A.S., Koons, P.O., Craw, D., Hallet, B., Chamberlain, C.P., Kidd, W.S.F., Park, S.K., Seeber, L., Bishop, M., Shroder, J., 2001. Erosion, Himalayan geodynamics, and the geomorphology of metamorphism. GSA Today 11, 4–9.

Zhang, H.P., Zhang, P.Z., Fan, Q.C., 2011. Initiation and recession of the fluvial knickpoints: A case study from the Yalu River-Wangtian'e volcanic region, northeastern China. Science China Earth Sciences 54, 1746–1753. doi:10.1007/s11430-011-4254-6